Conception of a test stand for Silicon Photomultipliers

von

Susanne Richer

Bachelorarbeit in Physik

vorgelegt der
Fakultät für Mathematik, Informatik und Naturwissenschaften der RWTH Aachen
im Juli 2010

angefertigt am
III. Physikalischen Institut A der RWTH Aachen
Prof. Dr. Thomas Hebbeker

Abstract

This thesis treats the conception of a tunable light source as a test stand for silicon photomultipliers. The main element is either a prism or a diffraction grating, used to disperse the light of a LED. A slit can be moved along the created spectrum, selecting a certain wavelength. A reference light source shall be used to calibrate the test stand, but is still in construction, as is the pulsed electronic for the LED. Apart from that, the test stand is working and ready for use. Both the version with the grating and the version with the prism work, even though the grating seems to be the better solution.
After introducing some theoretical prerequisites (refraction, diffraction, interference), prism and grating as the two main elements of the test stand are presented in detail. A simulation is used to demonstrate how light is dispersed by prisms. After these preparations the positions of the slit can be converted into their respective wavelengths.
In a first test measurement, the current in a PIN diode that is attached to the test stand is measured and plotted against the wavelength.

Zusammenfassung

Ziel dieser Bachelorarbeit ist die Konzeption einer durchstimmbaren Lichtquelle als Prüfstand für Silizium-Photomultiplier. Mit entweder einem Prisma oder einem Gitter wird das Licht einer LED in seine Bestandteile aufgespalten. Auf einem fahrbaren Schlitten kann ein Spalt entlang des Spektrums bewegt und so die Wellenlänge ausgesucht werden. Für die Eichung der Teststation soll eine Referenzlichtquelle verwendet werden, die aber genau wie die gepulste Elektronik für die LED noch in Konstruktion ist. Abgesehen davon ist die Teststation funktionstüchtig und einsatzbereit. Sowohl die Version mit dem Gitter, als auch die mit dem Prisma funktionieren, wobei das Gitter die bessere Lösung zu sein scheint.
Nach einigen theoretischen Grundlagen (Brechung, Beugung, Interferenz), werden Prisma und Gitter als Hauptbestandteile des Prüfstands im Detail vorgestellt. Dadurch wird es möglich, die Position des Spalts in die zugehörige Wellenlänge umzurechnen.
In einer ersten Testmessung wird der Strom in einer am Prüfstand angebrachten PIN-Diode gemessen und gegen die Wellenlänge aufgetragen.

Contents

1. Introduction

The intention of this thesis is to conceive and to construct a tunable light source as a test stand for silicon photomultipliers. Either a prism or a diffraction grating is used to split the light of a light-emitting diode into its components. Using a motorized stage, a slit can be moved along the created spectrum (see figure 1.1).

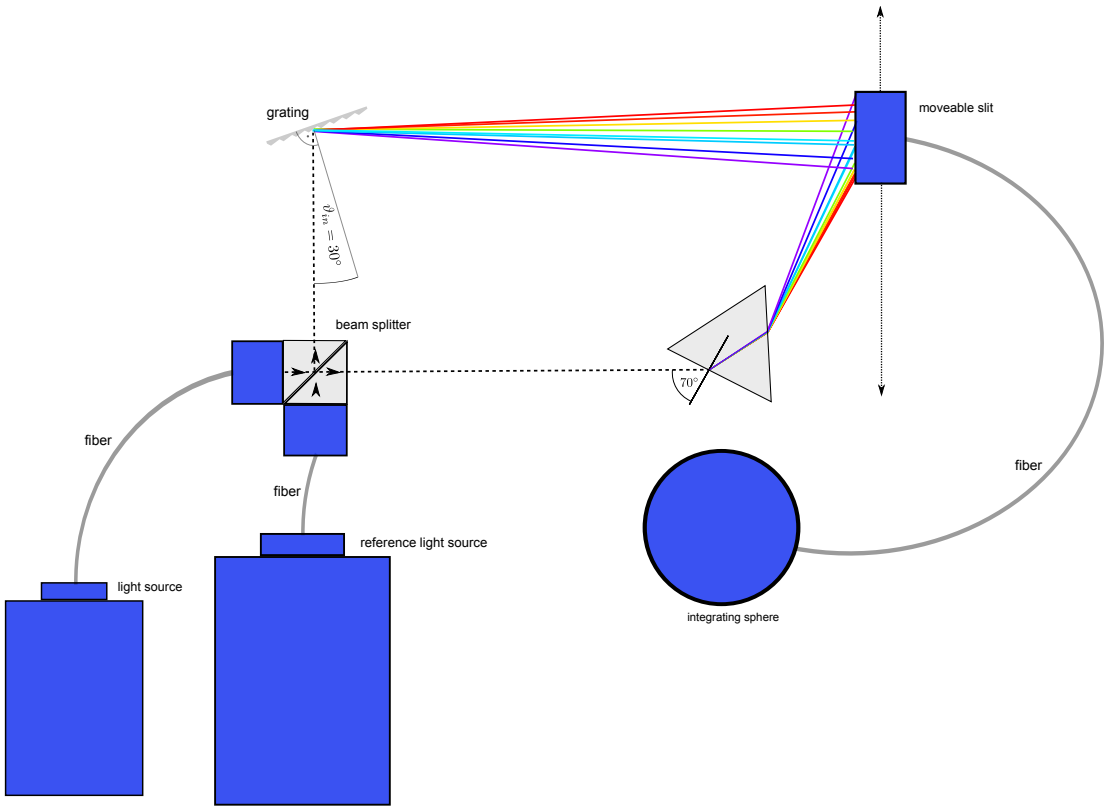

Figure 1.1.: Sketch of the set-up.

By calculations, the position of each wavelength in the spectrum can be determined. A reference light source containing four laser diodes of specific wavelengths shall be used to calibrate the tunable light source and to verify the calculations. The set-up also features an integrating sphere in which the light of the chosen wavelength is diffused before entering the silicon photomultiplier to be tested. In addition, a calibrated PIN diode for reference measuring is connected to the integrating sphere.
This project was conceived for two students. While this thesis concentrates on the theoretical conception (including some simulation) of the test stand, the other (see [4]) specializes in the practical construction.

2. Theoretical prerequisites

Visible light is electromagnetic radiation of a wavelength between about 380 nm and 780 nm. When the size of the structures with which the light interacts, is of the same order of magnitude as the wavelength, it has to be treated as a wave in order to explain effects like diffraction and interference. If, on the other hand, the wavelength is much smaller than the components it interacts with (like for example mirrors or prisms), the wavelike properties of light can be neglected. In this case, light propagation can be described in terms of rays. This simplification is called geometrical optics.

2.1. Reflection and refraction

When a ray of light strikes a boundary surface between two media, it will usually be both reflected and refracted (see figure 2.1).

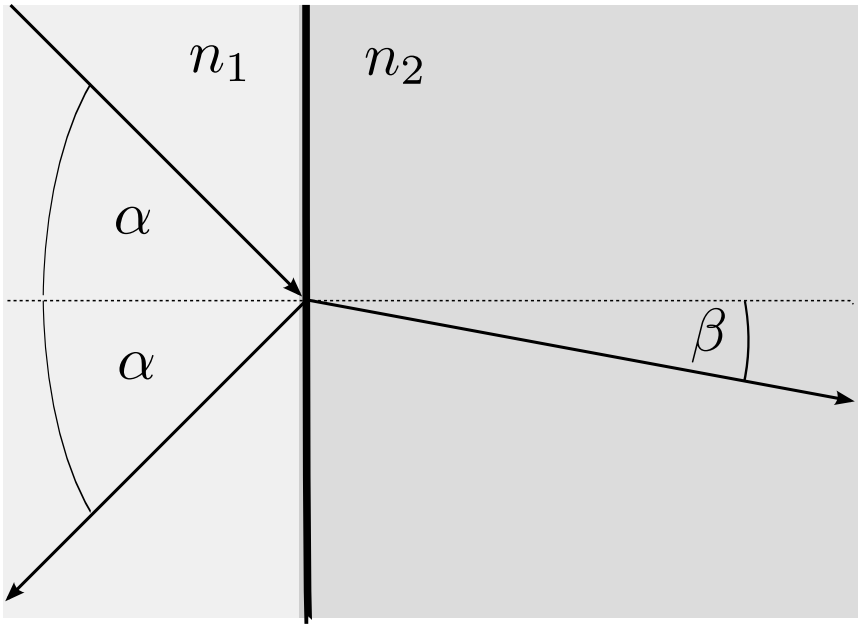

Figure 2.1.: A beam of light is both reflected and refracted on a boundary surface between two materials with different reflective indices n_1 and n_2.

The reflected ray makes the same angle α with the surface normal as the incident ray (see figure 2.1). The refracted ray bends according to Snell's law, which yields

$$n_1 \sin\alpha = n_2 \sin\beta, \tag{2.1}$$

where n_1 and n_2 are the refractive indices.

2.2. Interference and diffraction

In superpositions of waves the amplitudes add up according to their respective phases.

$$\vec{E}(\vec{r},t) = \sum_m \underbrace{\vec{A}_m(\vec{r},t)}_{\text{Amplitude}} \cdot \underbrace{e^{i\varphi_m}}_{\text{Phase}} \tag{2.2}$$

When the waves are in phase, i.e. $\varphi = n \cdot 2\pi$, the cumulative amplitude is maximal.

2.2.1. Multiple beam interference

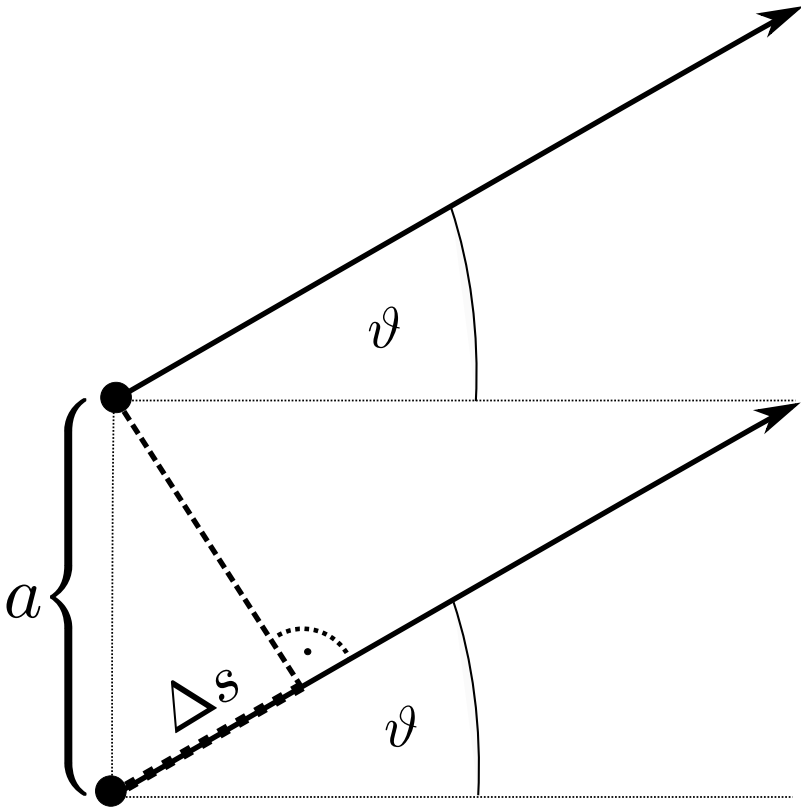

Figure 2.2.: Two beams of light at distance a have a path difference $\Delta s = a \sin\vartheta$, dependent on the viewing angle ϑ.

In case of N light beams with a distance a between each other, the phase difference between two adjacent beams is

$$\Delta\varphi = \frac{2\pi}{\lambda} \cdot \underbrace{a \sin\vartheta}_{\Delta s}. \tag{2.3}$$

Thus, the total electric field at a specific point is

$$E = A \sum_{k=1}^{N} e^{i(\omega t - \varphi_k)} = A e^{i\omega t} \sum_{k=1}^{N} e^{-i(k-1)\Delta\varphi}, \tag{2.4}$$

when the phase of the first partial wave is put equal to zero. Using the geometrical series

$$\sum_{j=0}^{n} x^j = \frac{1-x^n}{1-x} \qquad (\text{for } x \neq 0), \tag{2.5}$$

the electric field yields

$$E = Ae^{i\omega t}\frac{1-e^{-iN\Delta\varphi}}{1-e^{-i\Delta\varphi}} = Ae^{i\omega t}\frac{e^{-iN\frac{\Delta\varphi}{2}}(e^{iN\frac{\Delta\varphi}{2}}-e^{-iN\frac{\Delta\varphi}{2}})}{e^{-i\frac{\Delta\varphi}{2}}(e^{i\frac{\Delta\varphi}{2}}-e^{-i\frac{\Delta\varphi}{2}})}$$

$$= Ae^{i(\omega t-(N-1)\frac{\Delta\varphi}{2})}\frac{\sin(N\frac{\Delta\varphi}{2})}{\sin(\frac{\Delta\varphi}{2})}. \tag{2.6}$$

As the intensity I is proportional to E^2, it is

$$I = I_0\frac{\sin^2(N\pi\frac{a}{\lambda}\sin\vartheta)}{\sin^2(\pi\frac{a}{\lambda}\sin\vartheta)}. \tag{2.7}$$

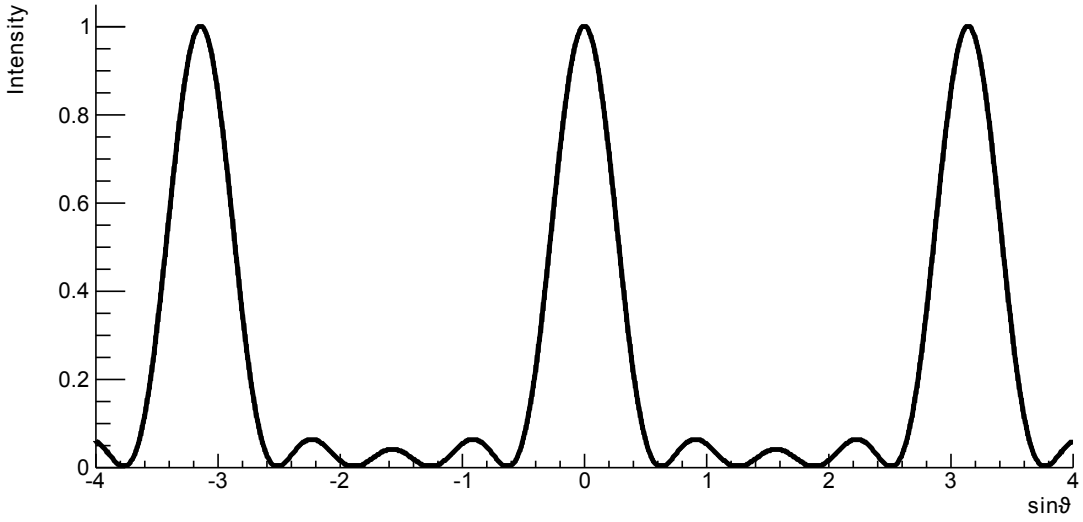

Figure 2.3.: Intensity pattern of multiple beam interference according to equation 2.7 (for $N = 5$, $\lambda = \pi a$ and $I_0 = 1$)

2.2.2. Single-slit diffraction

When a wave encounters an obstacle, it is bent and can thus reach regions behind the obstacle it could not reach according to geometrical optics.
According to Huygens' principle, each point of an advancing wave front is the starting point of a new wave. A wave front striking a narrow slit can thus be treated as multiple beam interference of many sources at a small distance. When the width of the slit is b, each beam is at a distance $a = \frac{b}{N}$ ($N >> 1$) to the adjacent ones. Therefore, the intensity yields

$$I = \tilde{I}_0\frac{\sin^2(N\pi\frac{a}{\lambda}\sin\vartheta)}{\sin^2(\pi\frac{a}{\lambda}\sin\vartheta)} = \tilde{I}_0\frac{\sin^2(\pi\frac{b}{\lambda}\sin\vartheta)}{\sin^2(\frac{1}{N}\underbrace{\pi\frac{b}{\lambda}\sin\vartheta}_{:=x})} = \tilde{I}_0\frac{\sin^2 x}{\sin^2(\frac{x}{N})}. \tag{2.8}$$

As the number of sources N in the slit tends to infinity, $\sin(\frac{x}{N})$ can be replaced with $\frac{x}{N}$ which yields

$$I = \underbrace{\tilde{I}_0 N^2}_{I_0} \frac{\sin^2 x}{x^2}. \tag{2.9}$$

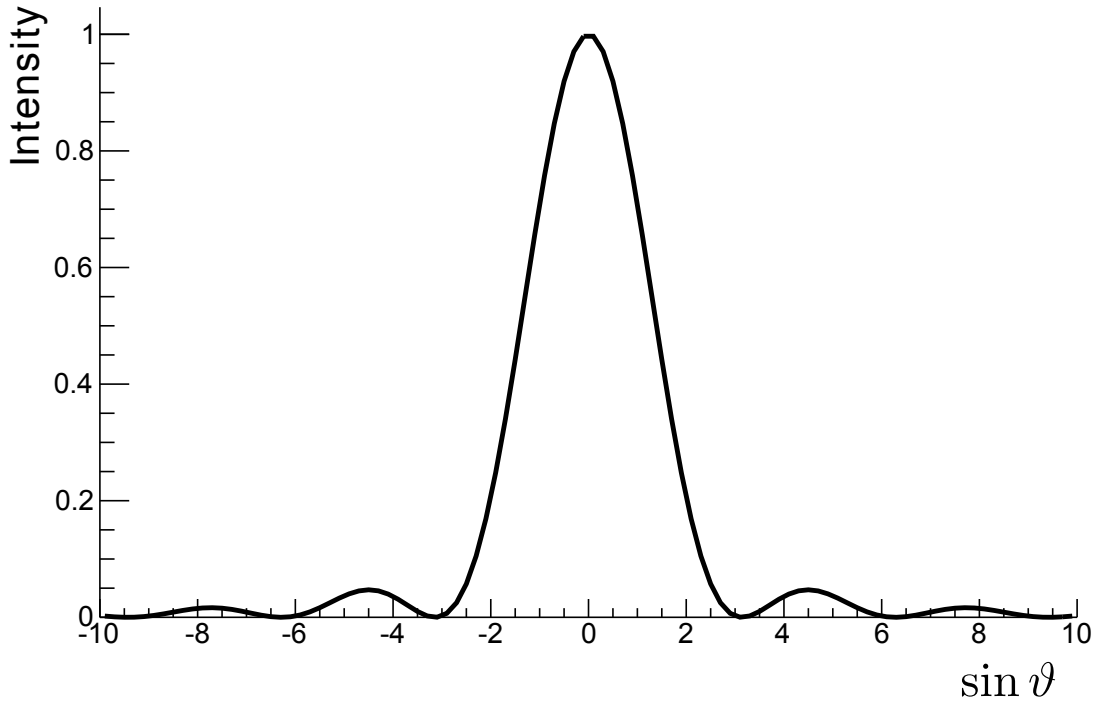

Figure 2.4.: Intensity pattern of single-slit diffraction according to equation 2.9 (for $\lambda = \pi b$ and $I_0 = 1$)

The zeroth maximum contains about 90 % of the intensity. The calculations in this section rely on [1].

3. Core Components

3.1. Prism

Optical prisms are instruments used to split light into its components. The prisms used in the scope of this thesis are equilateral prisms with a triangular base of 2 cm length and rectangular sides. The refractive index of the material is wavelength-dependent (dispersion). Thus, light of different wavelengths is refracted by different angles (see figure 3.1). Due to these different angles, the light leaving the prism is divergent.

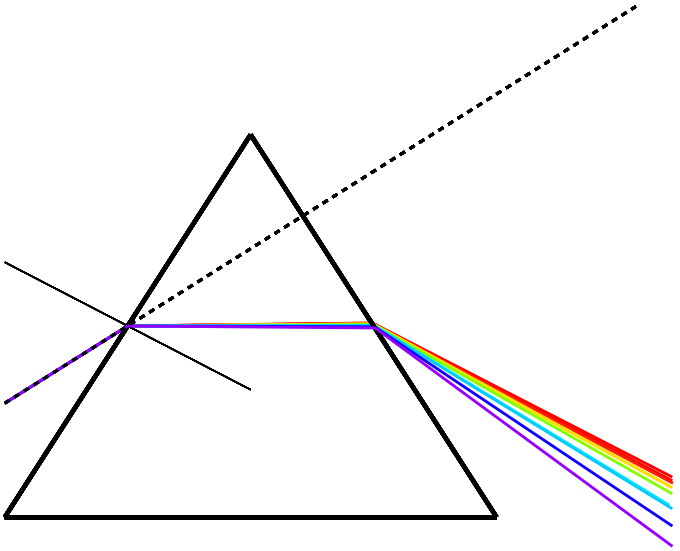

Figure 3.1.: Light traversing a prism.

Assuming that a prism is surrounded by air, it is $n_1 \approx 1$ and $n_2 = n$ in Snell's law (see equation 2.1). If the beam enters the prism at an angle $\beta_1 = \arcsin(\frac{1}{n} \sin \alpha_1)$ to the surface normal (where α_1 is the angle of incidence, see figure 3.2), it will strike the second surface at an angle $\beta_2 = \gamma - \beta_1$, where γ is the top angle of the prism. Thus, it leaves the prism at $\alpha_2 = \arcsin(n \sin \beta_2)$, while the total angle of deflection is δ.
In the red triangle it is

$$\begin{aligned} \pi &= (\pi - \delta) + (\alpha_1 - \beta_1) + (\alpha_2 - \beta_2) \\ &\Leftrightarrow \delta = \alpha_1 + \alpha_2 - (\beta_1 + \beta_2), \end{aligned} \tag{3.1}$$

while the green triangle yields

$$\begin{aligned} \pi &= \gamma + (\frac{\pi}{2} - \beta_1) + (\frac{\pi}{2} - \beta_2) \\ &\Leftrightarrow \gamma = \beta_1 + \beta_2, \end{aligned} \tag{3.2}$$

which leads to

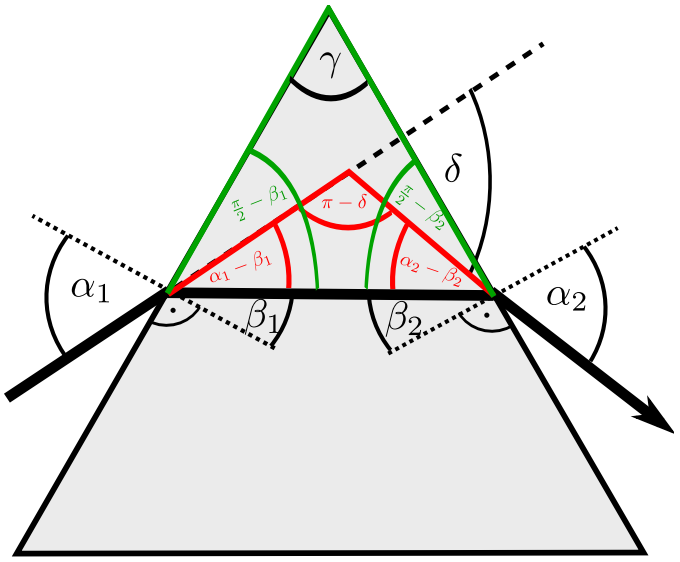

Figure 3.2.: The angle of total deflection δ depends on the prism opening angle γ, the incident angle α_1 and the refractive index of the glass (which depends on the wavelength).

$$\delta = \alpha_1 + \alpha_2 - \gamma = \alpha_1 - \gamma + \arcsin(n \sin \beta_2)$$

$$= \alpha_1 - \gamma + \arcsin(n \sin(\gamma - \beta_1))$$

$$= \alpha_1 - \gamma + \arcsin\left(n \sin\left(\gamma - \arcsin\left(\frac{1}{n} \sin \alpha_1\right)\right)\right). \tag{3.3}$$

Using

$$\sin(a - b) = \sin a \cdot \cos b - \cos a \cdot \sin b, \tag{3.4}$$

this yields

$$\delta = \alpha_1 - \gamma + \arcsin\left(n\left(\sin\gamma \cdot \cos\left(\arcsin\left(\frac{1}{n}\sin\alpha_1\right)\right) - \cos\gamma \cdot \frac{1}{n}\sin\alpha_1\right)\right), \tag{3.5}$$

and with

$$\cos(\arcsin x) = \sqrt{1 - x^2} \tag{3.6}$$

the total deflection in dependence of the incident angle α_1 is

$$\delta = \alpha_1 - \gamma + \arcsin(\sin\gamma \cdot \sqrt{n^2 - \sin^2\alpha_1} - \cos\gamma \cdot \sin\alpha_1). \tag{3.7}$$

Figure 3.3 illustrates the difference in the deflection angle δ across the spectrum, dependent on the opening angle γ of the prism and the incident angle α_1 according to equation 3.7.

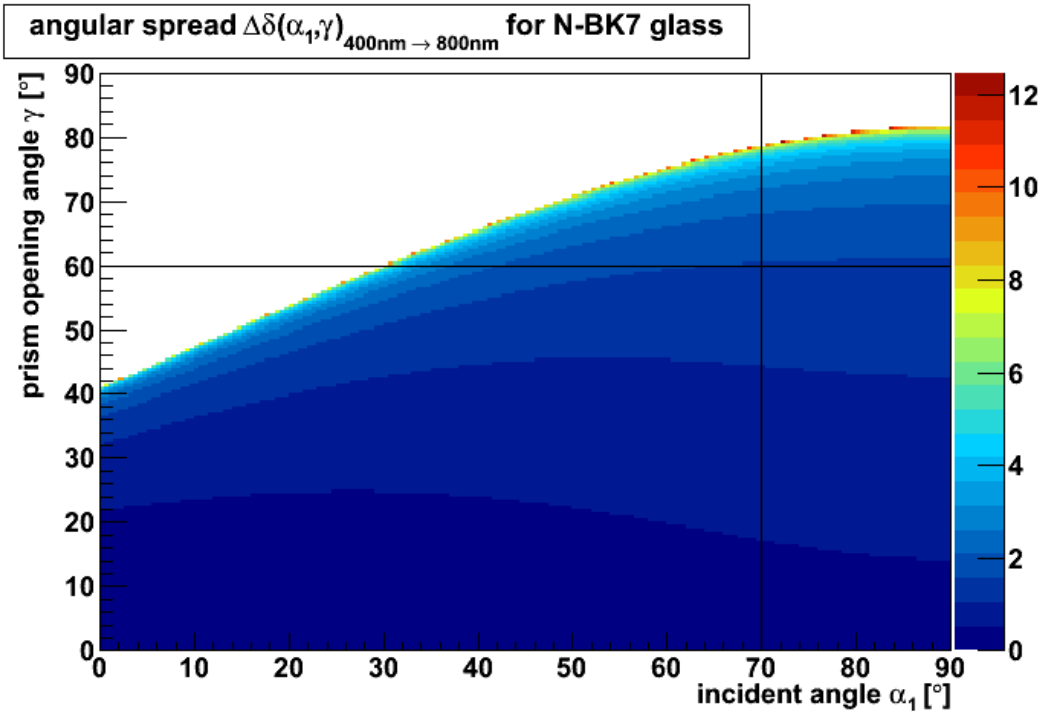

Figure 3.3.: The plot shows how the angle of deflection δ diverges between the edges of the spectrum (400 nm to 800 nm). The lines indicate the prism opening angle γ and incident angle α_1 used in the scope of this thesis. In the white area, there is total reflection for parts of the spectrum. The deflection is maximized at the border to this forbidden area.

3.1.1. Resolution

The resolution of a prism is

$$\frac{\lambda}{\Delta\lambda} = b \cdot \left|\frac{\mathrm{d}n}{\mathrm{d}\lambda}\right|, \tag{3.8}$$

where b is the length of the base of the prism (for the derivation see [3]). Figure 3.4 shows the derivation of the refractive index with regard to the wavelength, which is necessary for the resolution.
Thus, for an exemplary wavelength of $\lambda = 532\,\mathrm{nm}$ the resolution is

$$\frac{\lambda}{\Delta\lambda} = 0.02\,\mathrm{m} \cdot \frac{220000}{\mathrm{m}} = 4400, \tag{3.9}$$

which yields

$$\Delta\lambda = \frac{532\,\mathrm{nm}}{4400} = 0.121\,\mathrm{nm}. \tag{3.10}$$

This number indicates the theoretical upper limit of resolution. In reality, the resolution is additionally limited by the remaining divergence of the beam and the inexactness of other quantities (see section 4.1).

3.1.2. Combination of two prisms

After traversing a second prism, upside-down and parallel to the first one, the light becomes parallel to the incoming beam (see figure 3.5).

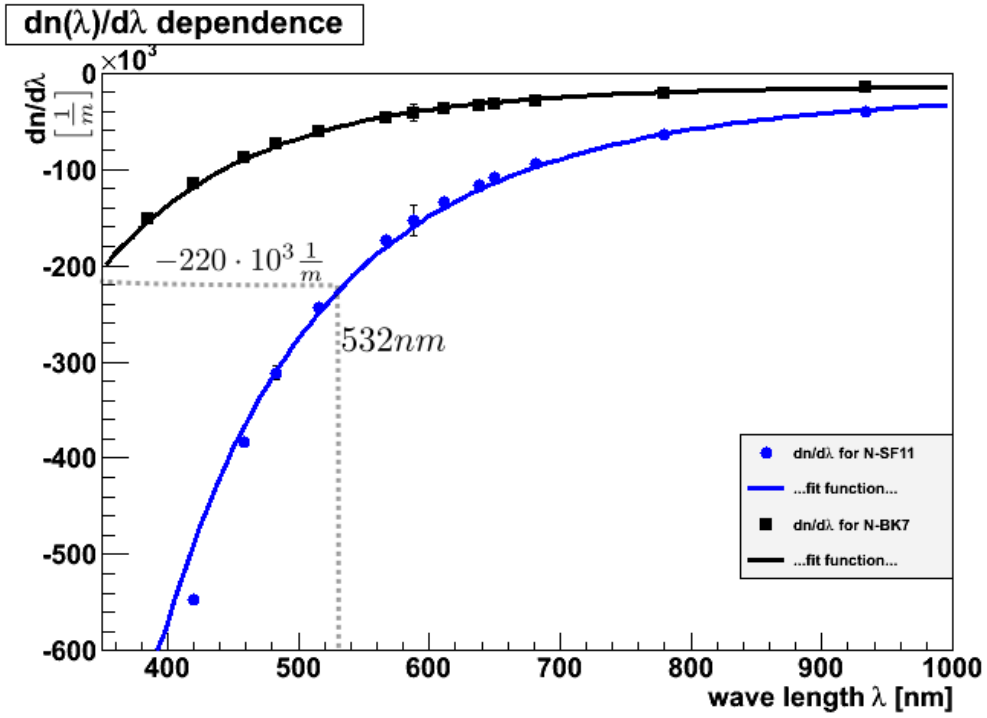

Figure 3.4.: The blue curve shows how the refractive index of N-SF11 glass depends on the wavelength. For comparison the black curve shows the same for N-BK7 glass. The prisms used in the scope of this thesis are made of N-SF11 glass.

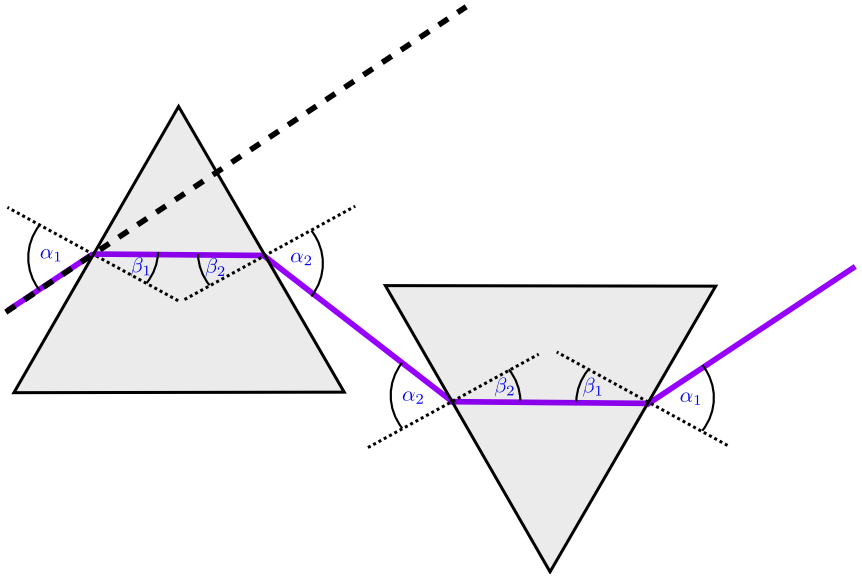

Figure 3.5.: A beam of light traversing two parallel prisms becomes parallel to the incoming beam.

As the second prism is parallel to the first, the light strikes the second prism at the same angle α_2 at which it left the first prism. It thus leaves the second prism at the incidence angle α_1 irrespective of the wavelength. As the outgoing spectrum is parallel to the incoming beam, a non-divergent spectrum can be produced by this arrangement.

3.2. Diffraction grating

A diffraction grating is a dispersive element with a periodic structure which is either transparent or reflective. The diffraction pattern behind the grating results from a superposition of single-slit diffraction and multiple beam interference (see figure 3.6).

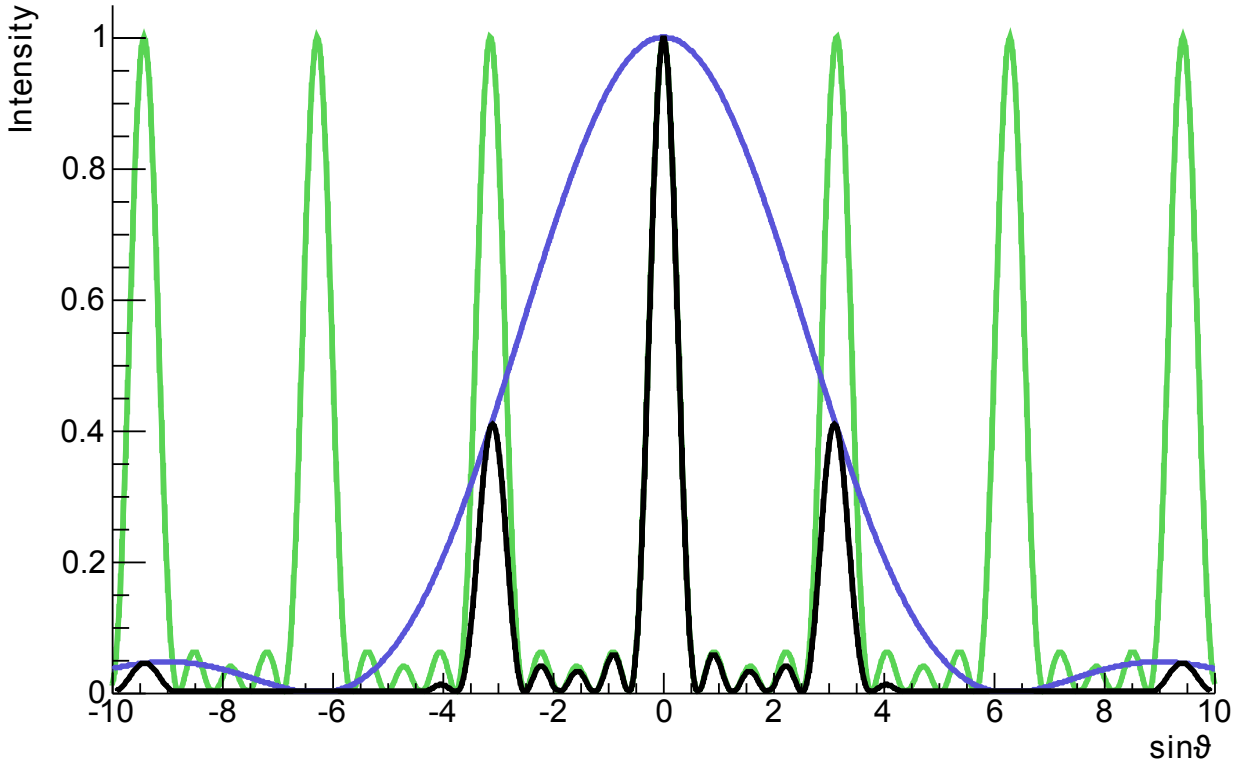

Figure 3.6.: The diffraction pattern of a grating (black curve) results from a multiplication of a diffraction term (blue) with an interference term (green), for $N = 5$, $d = 2b$ and $\lambda = \pi d$.

Therefore, the intensity yields

$$I = I_0 \cdot \underbrace{\frac{\sin^2(\pi \frac{b}{\lambda} \sin\vartheta)}{(\pi \frac{b}{\lambda} \sin\vartheta)^2}}_{\text{diffraction}} \cdot \underbrace{\frac{\sin^2(N\pi \frac{d}{\lambda} \sin\vartheta)}{\sin^2(\pi \frac{d}{\lambda} \sin\vartheta)}}_{\text{interference}}, \tag{3.11}$$

where b is the width of the slits, d the distance between two slits and ϑ the viewing angle (see figure 3.7).

The diffraction term peaks for $\pi \frac{b}{\lambda} \sin\vartheta = (2n+1)\frac{\pi}{2}$, the interference term for $\pi \frac{d}{\lambda} \sin\vartheta = m\pi$, where $m, n = 0, 1, 2...$ As the intensity is concentrated in the zeroth diffraction order, the interference maxima of higher orders are suppressed. While the zeroth order maximum is always at the same position, the positions of the other maxima are wavelength-dependent. Therefore, the zeroth maximum is white, while the different colours are separated in the maxima of higher orders. When an interference maximum coincides with a diffraction minimum (or vice versa), this maximum is annihilated. A disadvantage of conventional gratings is that most of the intensity is concentrated in the zeroth order, where the light is not split up.

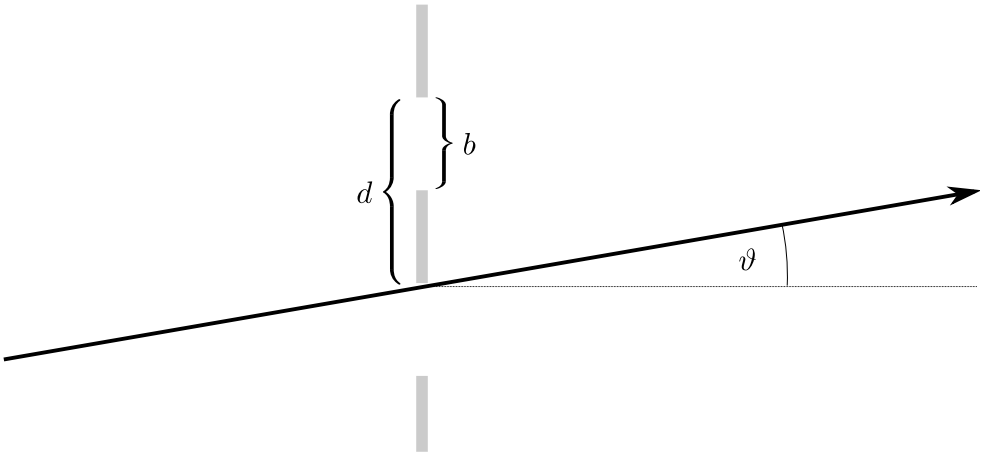

Figure 3.7.: Conventional grating, characterized by its slit width b and slit distance d.

3.2.1. Blazed grating

With a "blazed" grating, most of the intensity can be concentrated into the first interference order, by tuning the diffraction maximum to the first-order interference maximum. Blazed gratings are reflective gratings, characterized by their period d and by the inclination γ of the facets respective to the horizontal (see figure 3.8).

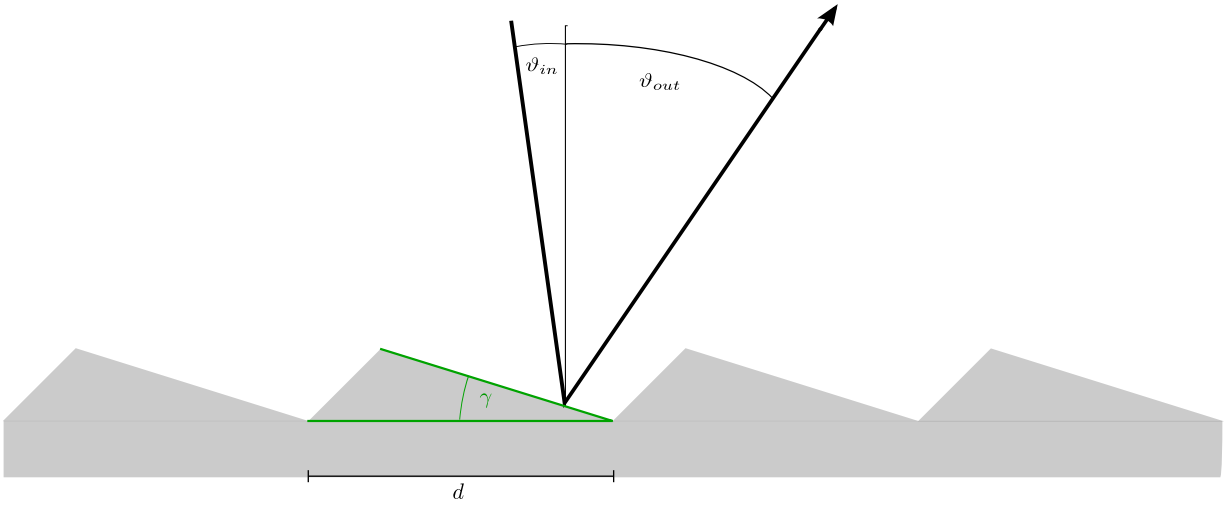

Figure 3.8.: Blazed grating, characterized by its period d and facet inclination γ.

Here, too, the pattern produced by the grating results from the superposition of a diffraction term (superposition of beams hitting the same facet at different positions) with an interference term (beams hitting different facets at the same relative position).
In order to calculate the first term, it is necessary to determine the phase shift between two beams hitting the same facet at a distance x, assuming that the first one hits the facets at the start of a period. The following calculations are similar to [8].
As can be seen in figure 3.9, beam 1 travels a distance Δl_1 longer than beam 2 before hitting the facet. In the red triangle, it is $\Delta l_1 = \tilde{x} \cdot \cos\epsilon_1$, with $\vartheta_{in} + \epsilon_1 + \gamma = \frac{\pi}{2}$ and $\tilde{x} = \frac{x}{\cos\gamma}$ (green triangle). Therefore it is

$$\Delta l_1 = \frac{x}{\cos\gamma} \cdot \cos\left(\frac{\pi}{2} - \vartheta_{in} - \gamma\right) = \frac{x}{\cos\gamma} \cdot \sin(\vartheta_{in} + \gamma). \tag{3.12}$$

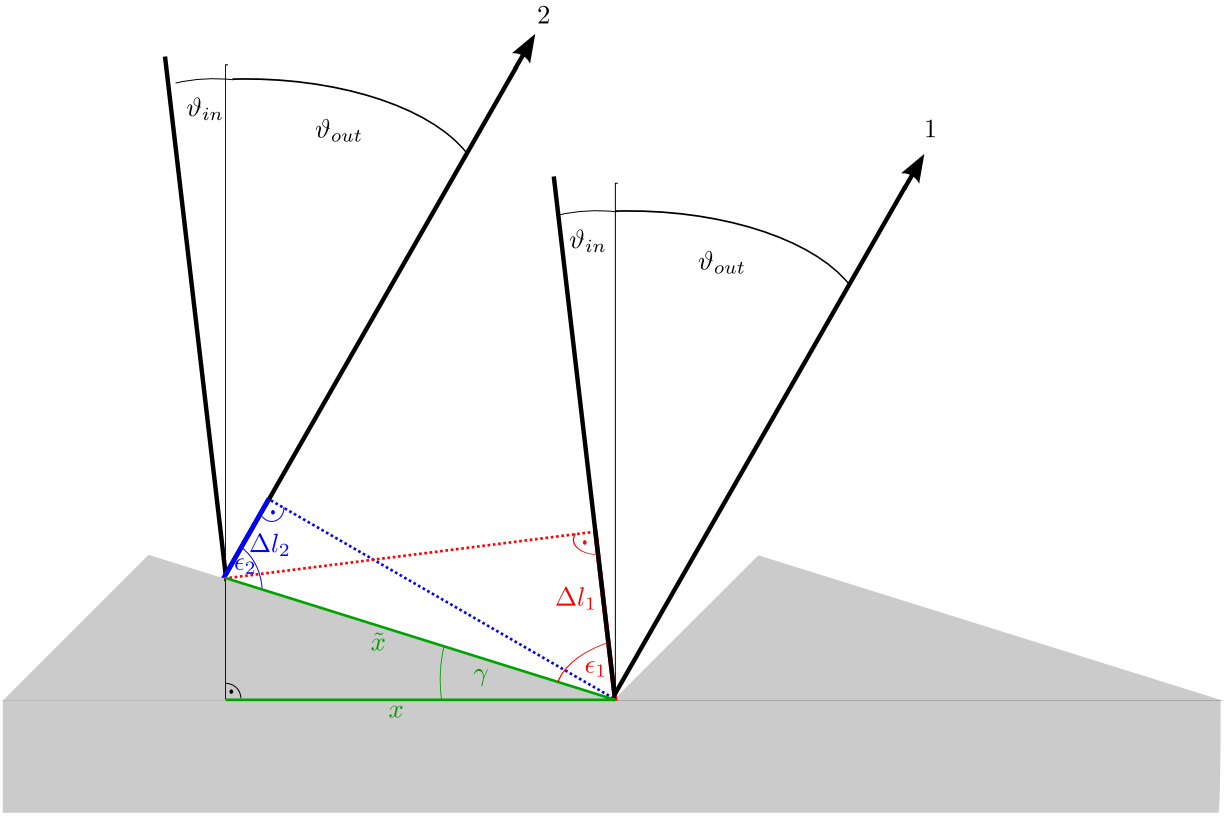

Figure 3.9.: Two parallel beams of light hit the same facet with an incident angle ϑ_{in} to the normal of the grating (not the facet normal). They leave the grating with the same angle ϑ_{out}.

After hitting the facet, beam 2 travels a distance Δl_2 longer than beam 1. In the blue triangle it is $\Delta l_2 = \tilde{x} \cdot \cos\epsilon_2$, with $\vartheta_{out} + \epsilon_2 + (\frac{\pi}{2} - \gamma) = \pi$, which yields

$$\Delta l_2 = \frac{x}{\cos\gamma} \cdot \cos\left(\frac{\pi}{2} - \vartheta_{out} + \gamma\right) = -\frac{x}{\cos\gamma} \cdot \sin(\vartheta_{out} - \gamma). \tag{3.13}$$

The phase shift between the two beams is

$$\varphi_I(x) = \frac{2\pi}{\lambda} \cdot (\Delta l_1 - \Delta l_2) = \frac{2\pi x}{\lambda \cos\gamma}(\sin(\vartheta_{in} + \gamma) - \sin(\vartheta_{out} - \gamma)). \tag{3.14}$$

Using

$$\sin a - \sin b = 2\cos\left(\frac{a+b}{2}\right)\sin\left(\frac{a-b}{2}\right) \tag{3.15}$$

(with $a = \vartheta_{in} + \gamma$ and $b = \vartheta_{out} - \gamma$), this yields

$$\begin{aligned}\varphi_I(x) &= \frac{4\pi x}{\lambda\cos\gamma}\cos\left(\underbrace{\frac{\vartheta_{out} + \vartheta_{in}}{2}}_{:=\alpha}\right)\sin\left(\gamma - \underbrace{\frac{\vartheta_{out} - \vartheta_{in}}{2}}_{:=\beta}\right) \\ &= \frac{4\pi x}{\lambda\cos\gamma}\cos\alpha\sin(\gamma - \beta).\end{aligned} \tag{3.16}$$

Figure 3.10 shows two beams hitting two adjacent facets at the same relative position. Their phase shift is $\varphi_{II} = \frac{2\pi}{\lambda}(\Delta s_1 - \Delta s_2)$, where $\Delta s_1 = d\sin\vartheta_{in}$ is the distance beam 1

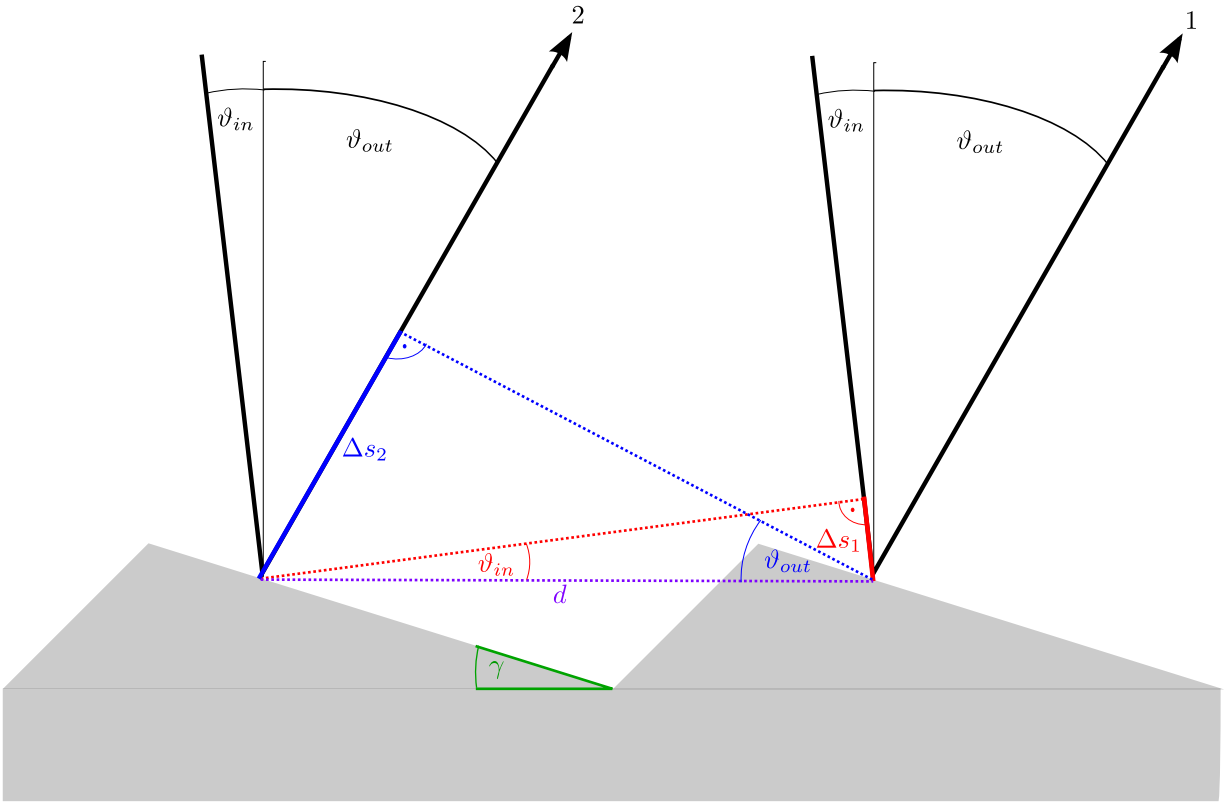

Figure 3.10.: Two beams of parallel beams of light hitting adjacent facets.

travels longer than beam 2 before hitting the facet, while $\Delta s_2 = d \sin \vartheta_{out}$ is the distance beam 2 travels longer than beam 1 after hitting the facet. Thus the phase shift yields

$$\varphi_{II} = \frac{2\pi d}{\lambda}(\sin \vartheta_{in} - \sin \vartheta_{out}) = \frac{4\pi d}{\lambda} \cos \alpha \sin(-\beta) \tag{3.17}$$

again using equation 3.15. By integrating over all positions x on a facet and summing up all facets N, the total electric field $E \propto e^{i(\omega t + \varphi_{ges})}$ can be calculated:

$$E \propto \sum_{n=1}^{N} \int_0^d e^{i(\omega t + \varphi_I(x) + n\varphi_{II})}\, dx = e^{i\omega t} \sum_{n=1}^{N} \int_0^d e^{i(\varphi_I(x) + n\varphi_{II})}\, dx \tag{3.18}$$

Abbreviating $\varphi_I(x) = \underbrace{\frac{4\pi}{\lambda \cos \gamma} \cos \alpha \sin(\gamma - \beta)}_{:=\varphi_0} \cdot x = \varphi_0 \cdot x$, this yields

$$E \propto e^{i\omega t} \int_0^d e^{i\varphi_0 x}\, dx \sum_{n=1}^{N} e^{in\varphi_{II}} = e^{i\omega t} \left. \frac{e^{i\varphi_0 x}}{i\varphi_0} \right|_0^d \underbrace{\sum_{n=1}^{N} e^{in\varphi_{II}}}_{\text{geometrical series}}$$

$$= e^{i\omega t} \frac{e^{i\varphi_0 d} - 1}{i\varphi_0} \cdot \frac{e^{iN\varphi_{II}} - 1}{e^{i\varphi_{II}} - 1}. \tag{3.19}$$

Thus, the intensity $I \propto E$ is

$$I(\alpha, \beta) = \tilde{I}_0 \frac{e^{i\varphi_0 d} - 1}{i\varphi_0} \cdot \frac{e^{-i\varphi_0 d} - 1}{-i\varphi_0} \cdot \frac{e^{iN\varphi_{II}} - 1}{e^{i\varphi_{II}} - 1} \cdot \frac{e^{-iN\varphi_{II}} - 1}{e^{-i\varphi_{II}} - 1}$$

$$= \underbrace{\tilde{I}_0 d^2}_{I_0} \left(\frac{\sin(\frac{\varphi_0 d}{2})}{\frac{\varphi_0 d}{2}} \right)^2 \cdot \left(\frac{\sin(\frac{N\varphi_{II}}{2})}{\sin(\frac{\varphi_{II}}{2})} \right)^2$$

$$= I_0 \underbrace{\left(\frac{\sin(\frac{2\pi d}{\lambda \cos\gamma} \cos\alpha \sin(\gamma - \beta))}{\frac{2\pi d}{\lambda \cos\gamma} \cos\alpha \sin(\gamma - \beta)} \right)^2}_{\text{diffraction}} \cdot \underbrace{\left(\frac{\sin(\frac{2\pi N d}{\lambda} \cos\alpha \sin\beta)}{\sin(\frac{2\pi d}{\lambda} \cos\alpha \sin\beta)} \right)^2}_{\text{interference}}. \tag{3.20}$$

The second term corresponds to the multiple beam interference term derived in section 2.2.1. The first term, which corresponds to the single-slit diffraction term from section 2.2.2, modulates the intensity. The special characteristic of a blazed grating is that the diffraction term peaks at the first order maximum of the interference term. The diffraction term peaks as its denominator tends to zero, which happens when

$$\frac{2\pi d}{\lambda \cos\gamma} \cos\alpha \sin(\gamma - \beta) = 0. \tag{3.21}$$

Supposing that α is smaller than $\frac{\pi}{2}$, the only possibility to fulfil this is $\sin(\gamma - \beta) = 0$, which corresponds to $\beta = \gamma$ as neither β nor γ can be larger than $\frac{\pi}{2}$. Substituting this into $\beta = \frac{\vartheta_{out} - \vartheta_{in}}{2}$ yields

$$\vartheta_{out} - \vartheta_{in} = 2\gamma \Leftrightarrow \vartheta_{in} + \gamma = \vartheta_{out} - \gamma, \tag{3.22}$$

which is the condition for specular reflection at the facets (see figure 3.11).

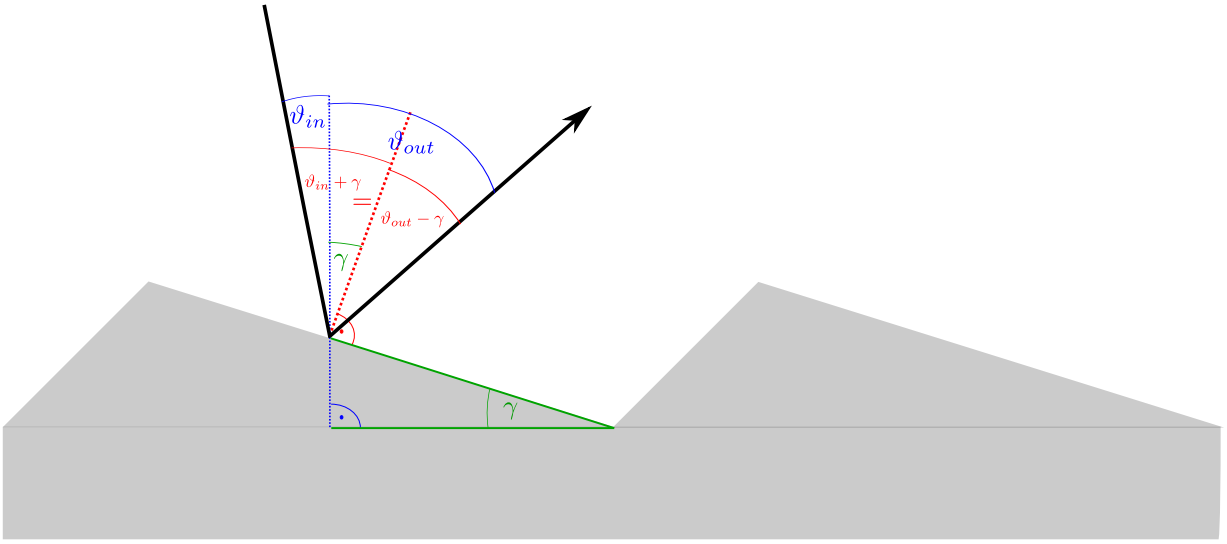

Figure 3.11.: In case of specular reflection respective to the facets, maximum intensity is achieved.

The maximum of the diffraction term, which corresponds to maximum intensity, is therefore achieved when the reflection at the facet is specular. The maximum intensity of a blazed grating coincides with the first-order interference maximum, which is at

$$\frac{2\pi d}{\lambda} \cos\alpha \sin\beta = m\pi \tag{3.23}$$

with $m = 1$ for the first maximum. Both conditions can be fulfilled for one particular wavelength λ, called blaze-wavelength

$$\lambda_b = 2d\cos\alpha\sin\gamma = 2d\cos\left(\frac{\vartheta_{out}+\vartheta_{in}}{2}\right)\sin\gamma = 2d\cos\left(\vartheta_{in}+\gamma\right)\sin\gamma. \tag{3.24}$$

3.2.2. Resolution

According to the Rayleigh criterion, two light sources can be resolved, when the distance between their principal maxima is at least as great as the distance between the maximum and the first minimum. This condition is satisfied for two sources of different wavelengths, when the a maximum of one wavelength coincides with the adjacent minimum of the other. This yields

$$\frac{\lambda}{\Delta\lambda} = mN \tag{3.25}$$

(for the derivation see [3]), where $m = 1$ is the order of maximum and N the number of illuminated facets. The spot of light on the grating has a diameter of approximately 7 mm, the period of the blazed grating used in the scope of this thesis is $d = \frac{600}{\text{mm}}$, which yields for the resolution

$$\frac{\lambda}{\Delta\lambda} = N = 7\,\text{mm}\cdot\frac{600}{\text{mm}} = 4200, \tag{3.26}$$

which is of the same order of magnitude as the resolution of the prism (see equation 3.9). Thus, for a wavelength of $\lambda = 532\,\text{nm}$ it is

$$\Delta\lambda = \frac{532\,\text{nm}}{4200} = 0.127\,\text{nm}. \tag{3.27}$$

Just as for the prism, this theoretical resolution is limited by the inexactness of the measured quantities (see section 4.2). For more information on (blazed) gratings see [2] and [5].

3.3. Integrating Sphere

An integrating sphere is an optical instrument used to disperse light uniformly. It consists of a spherical cavity coated with a highly reflective material with small openings for light entrance and exit (see figure 3.12(a)). By multiple reflections, the directions of the light are almost equally distributed.

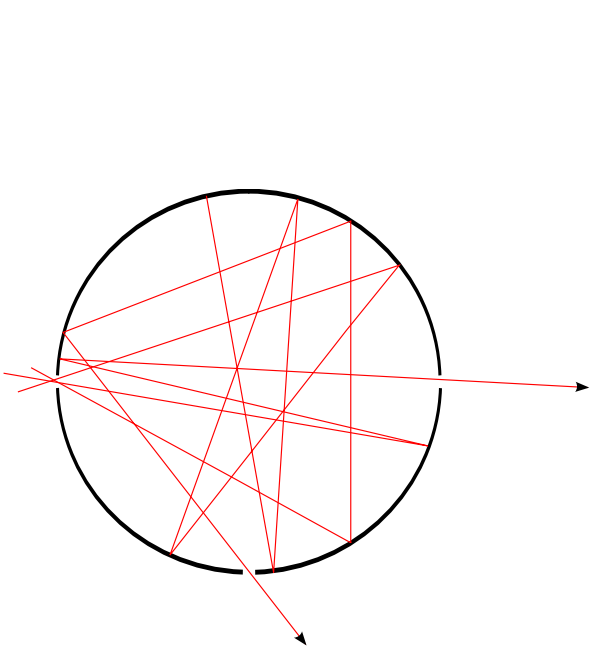

(a) Scheme showing the operation mode of an integrating sphere.

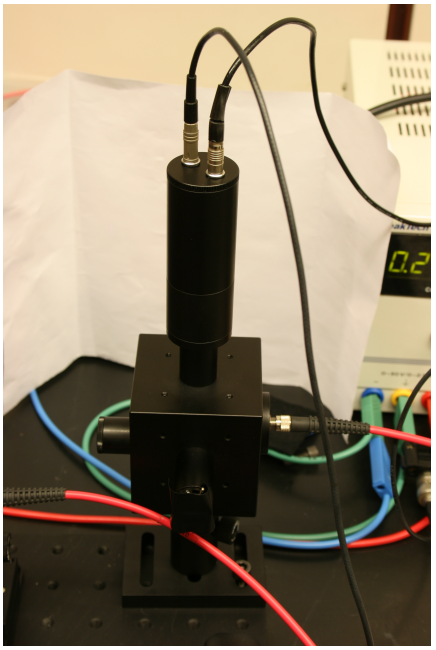

(b) The integrating sphere in the set-up with the PIN diode used for reference measuring.

Figure 3.12.: Integrating spheres.

The apertures have to be small compared to the inner surface of the sphere in order to ensure, that the light only leaves the sphere after many reflections. For further information on integrating spheres see [7].
In the set-up, the light enters the integrating sphere through an optical fiber (on the right side in figure 3.12(b)). A calibrated PIN diode used for reference measurements (see section 5) and the photomultiplier to be tested are attached to the exit apertures. A similar set-up was already used in a previous bachelor thesis (see [6]).

4. Conception of the test stand

In order to construct a tunable light source, the light of a light-emitting diode containing the whole visible spectrum, is split into its spectral components using either a blazed grating (see section 3.2.1) or a prism (see section 3.1) as dispersive element. In order to pick a certain wavelength, a slit is positioned on a motorized stage, which can be moved along the spectrum. After traversing an optical fiber, the light is diffused in an integrating sphere (see section 3.3).

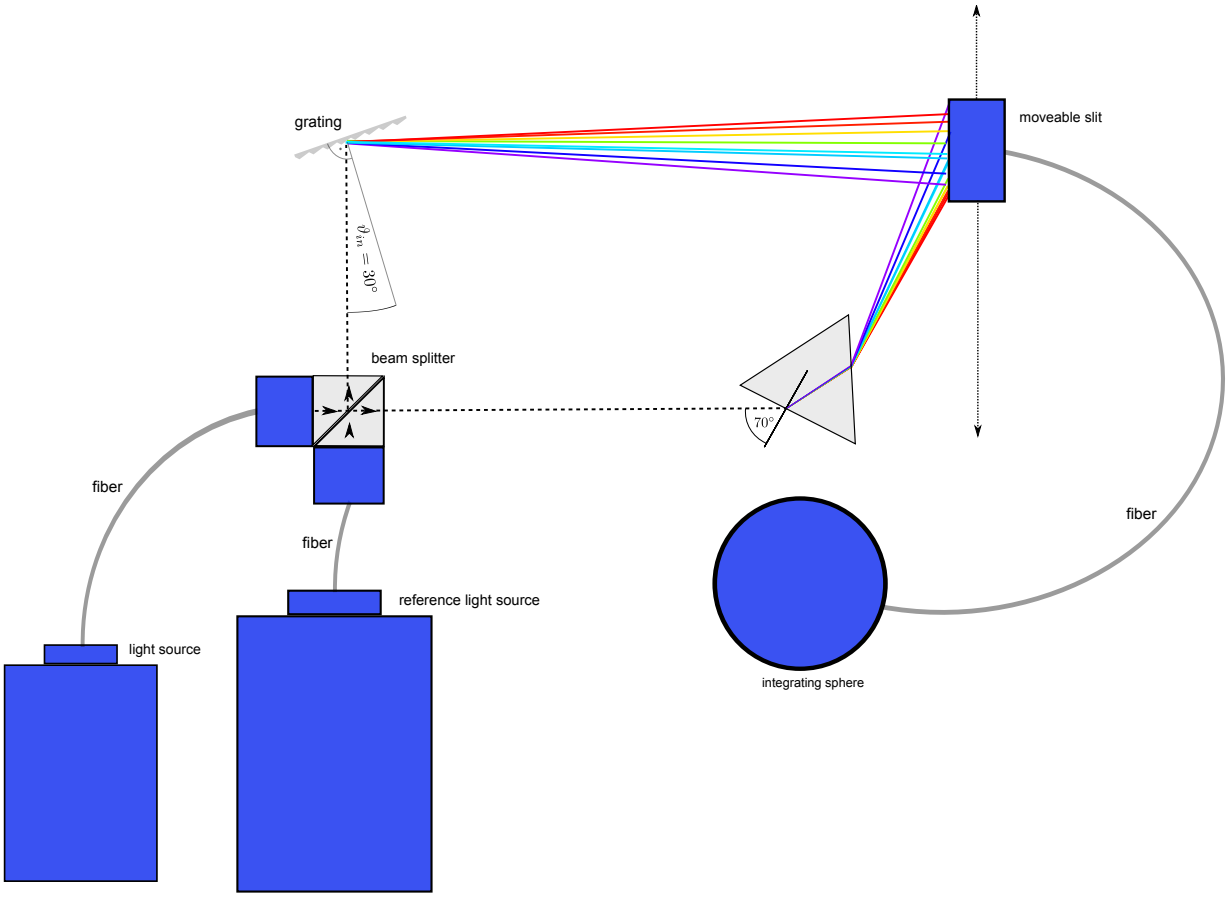

Figure 4.1.: Sketch of the set-up.

The set-up also features a reference light source, consisting of four laser diodes of different wavelengths (405 nm, 532 nm, 635 nm, 670 nm). Their light goes the same way as the laser diodes' light, producing four discrete points instead of a spectrum. Knowing the wavelengths of the laser diodes, the tunable light source can thus be calibrated, in order to verify the following calculations (see sections 4.1 and 4.2).
The set-up is designed and constructed in such a way as to enable an easy exchange between prisms and grating (see figure 4.1).

4.1. Using a prism

The equilateral prisms used in the scope of this thesis are made of N-SF11 glass, the sides are 2 cm long. There are several possibilities to disperse light using different combinations of prisms. With a C++-simulation using ROOT libraries, the path of a beam of light striking prisms or mirrors is calculated and displayed. The routine searches for the nearest intersection point of a light beam with a prism side (or a mirror), then decides by which angle to turn due to reflection and refraction law (see figure 4.2). Thus, the position of each wavelength in the spectrum can be determined, dependent on the wavelength (for more simulation plots see section D). The simulation features eleven different wavelengths between 404.7 nm and 706.5 nm with their respective refractive indices, as displayed in table C.1.

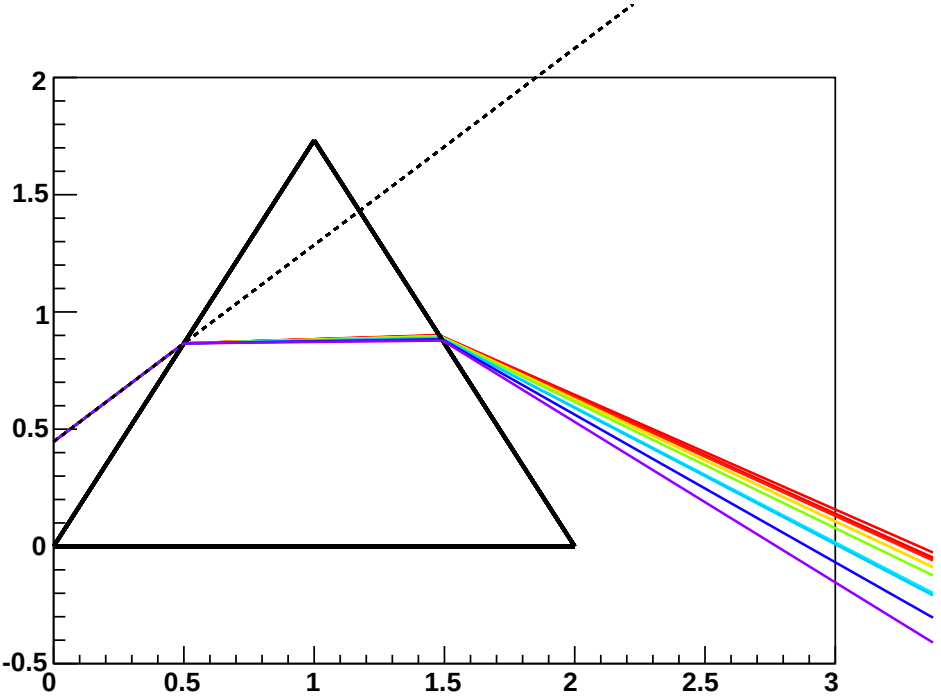

Figure 4.2.: The simulation shows how a beam of light is dispersed by a single prism.

At an incident angle of 70°, the angle of total deflection δ (see figure 4.3) varies between $\delta = 66.0°$ for a wavelength $\lambda = 706.5\,\text{nm}$ (red beam) and $\delta = 74.2°$ for $\lambda = 404.7\,\text{nm}$ (violet beam), which makes $\Delta\delta = 8.2°$. Thus, at a distance d from the prism, the width x of the spectrum is

$$\tan\left(\frac{\Delta\delta}{2}\right) = \frac{\frac{x}{2}}{d}$$

$$\Leftrightarrow x = 2d\tan\left(\frac{\Delta\delta}{2}\right). \tag{4.1}$$

In the set-up, however, the slit is not placed parallel to the spectrum of the prism, in order to find the prism spectrum at the same position as the spectrum of the grating (see again figure 4.1).
The slit moves perpendicularly to the incoming beam and the extension of its track passes the point where the light leaves the prism (which is approximately the same for all wavelengths) at a minimum distance of 6.3 cm. The angle of total deflection is

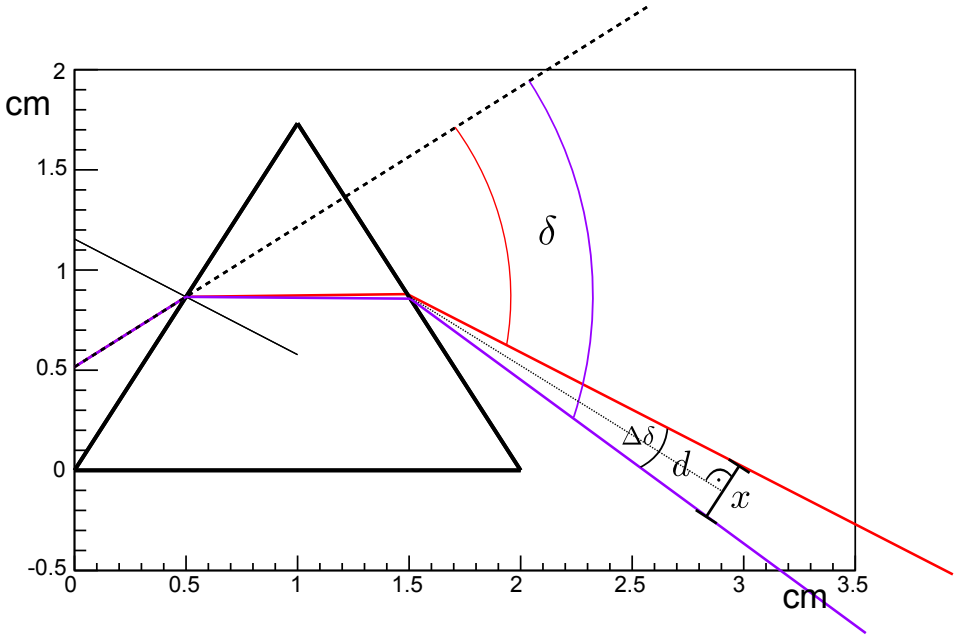

Figure 4.3.: The smaller the wavelength, the greater the deflection angle δ.

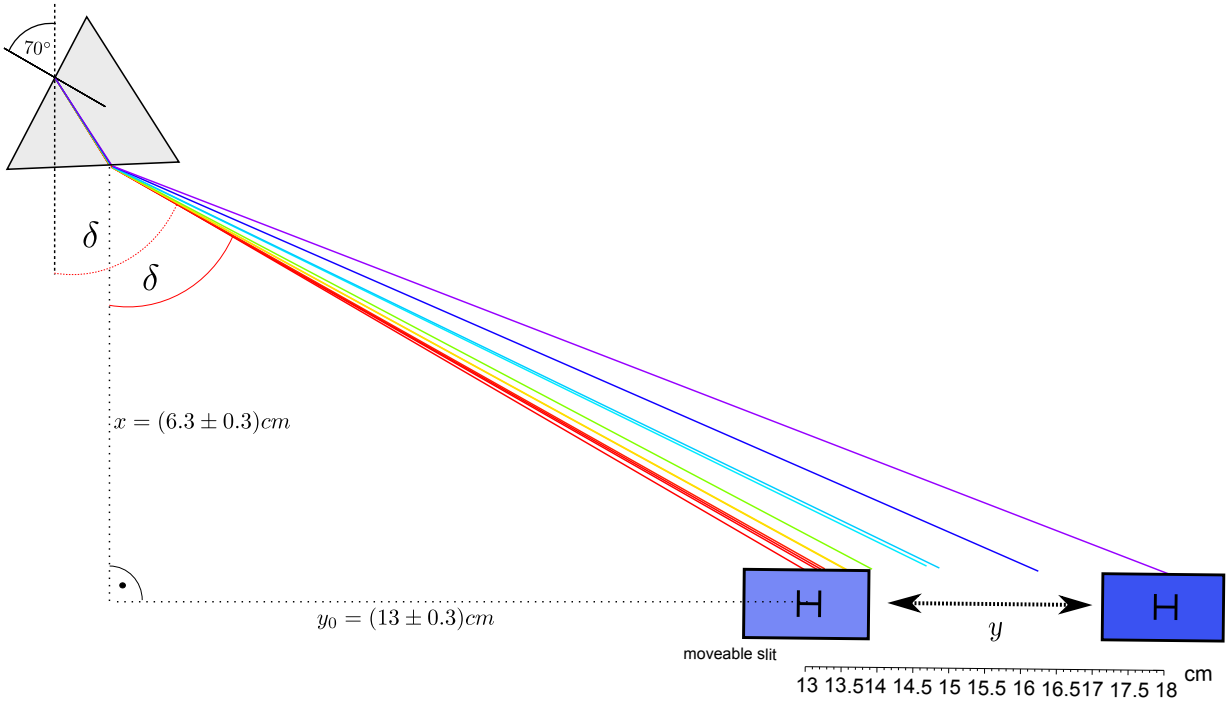

Figure 4.4.: Rotated detail from figure 4.1. The slit can be moved along a distance of 5 cm perpendicularly to the incoming beam.

$$\delta = \arctan\left(\frac{y}{x}\right), \tag{4.2}$$

as can be seen in figure 4.4. The deflection angle δ depends on the refractive index n according to equation 3.7. Table C.1 shows how the refractive index of N-SF11 glass varies with the wavelength, as indicated by the manufacturer of the prisms. In figure 4.5 a list of calculated deflection angles δ is plotted against their respective wavelengths.
A fit to the data, yields

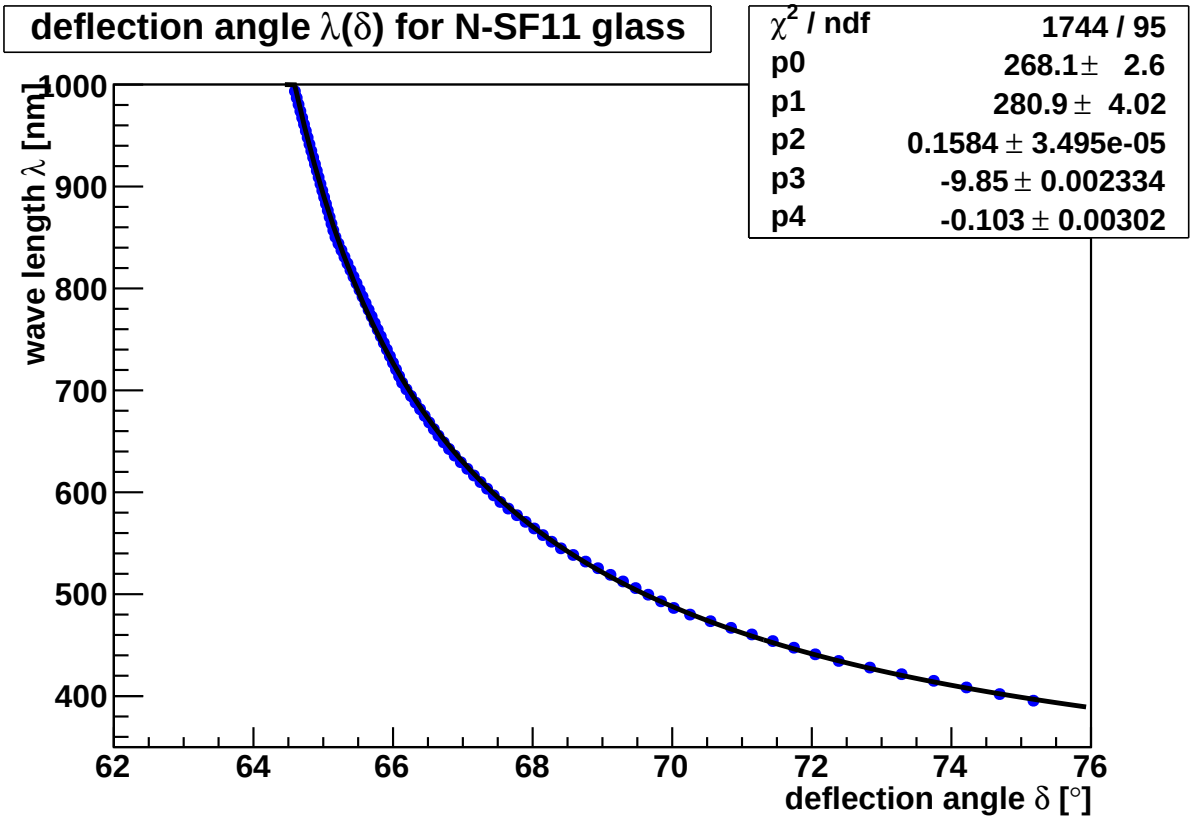

Figure 4.5.: The plot shows the dependence of the wavelength λ on the deflection angle δ with a fit function as per equation 4.3.

$$\lambda(\delta) = p_0 + \frac{p_1}{p_2\delta + p_3} + p_4\delta \tag{4.3}$$

and inserting equation 4.2 it is

$$\lambda(y) = p_0 + \frac{p_1}{p_2 \cdot \arctan\left(\frac{y}{x}\right) + p_3} + p_4 \cdot \arctan\left(\frac{y}{x}\right). \tag{4.4}$$

Using equation 4.4, the slit position can now be converted into the corresponding wavelength. The errors on x and y propagate into the error on δ according to

$$\sigma_\delta = \sqrt{\left(\frac{xy}{x^2+y^2}\right)^2 \cdot \left[\left(\frac{\sigma_y}{y}\right)^2 + \left(\frac{\sigma_x}{x}\right)^2\right]}, \tag{4.5}$$

while σ_δ propagates on the error on the wavelength σ_λ. For $x = (6.3 \pm 0.3)$ cm and $y = (18 \pm 0.3)$ cm (maximum value) it is $\delta_{max} = (70.7 \pm 0.9)°$, while for $y = (13 \pm 0.2)$ cm (minimum value), it is $\delta_{min} = (64.1 \pm 1.2)°$. Error propagation yields

$$\sigma_\lambda = \sqrt{\left(\frac{-p_1 p_2}{(p_2 \cdot \delta + p_3)^2} + p_4\right)^2} \cdot \sigma_\delta, \tag{4.6}$$

which leads to $\lambda_{min}(\delta_{max}) = (456.5 \pm 17.1)$ nm and $\lambda_{max}(\delta_{min}) = (817.8 \pm 190.6)$ nm respectively. As the error rises with the wavelength, it is calculated for different y-ranges to be used later on in the measurement plots (see section 5).

4.2. Using a grating

The spectrum produced by the grating looks better than the one produced by the prisms and has a higher intensity. The grating is also easier to handle. Therefore, it is the first choice for the set-up, the prism being the alternative.
The blazed grating used in the set-up has 600 lines per mm, which yields for its period $d = \frac{1\,\text{mm}}{600} = 1.667\,\mu\text{m}$. The facet inclination is $\gamma = 8° 37'$ and the blaze-wavelength $\lambda_b = 500\,\text{nm}$. According to equation 3.22, there is specular reflection for light of blaze-wavelength λ_b. Thus, for a fixed incident angle ϑ_{in}, light of λ_b will be found at an angle $\vartheta_{out} = \vartheta_{in} + 2\gamma$. For other wavelengths, the observation angles (first-order maximum) can be calculated from equation 3.23. Recasting yields

$$\lambda = d(\sin\vartheta_{out} - \sin\vartheta_{in}). \tag{4.7}$$

(for the calculation see section B).

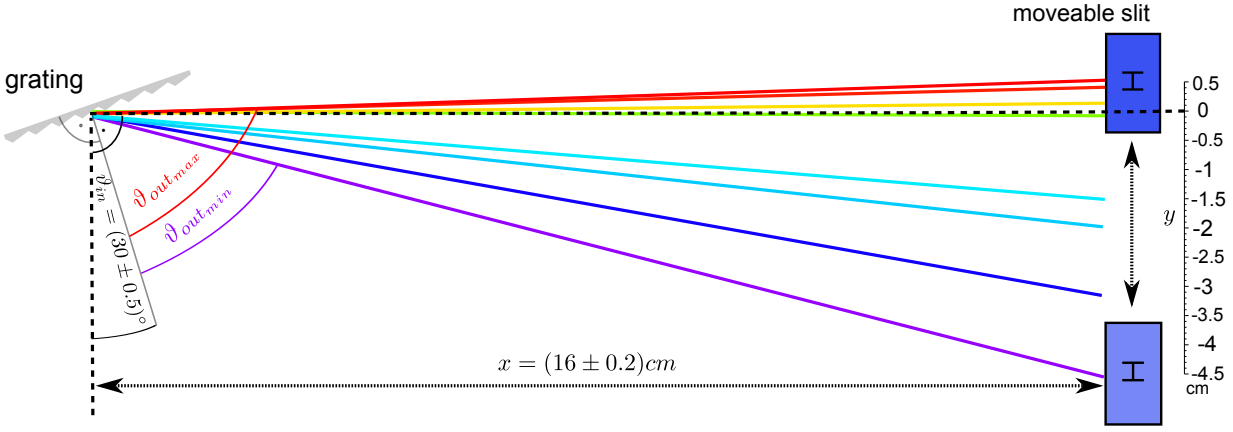

Figure 4.6.: detail from figure 4.1

As can be seen in figure 4.6, the slit can be moved along a distance of 5 cm. The observing angle is

$$\vartheta_{out} = \frac{\pi}{2} - \vartheta_{in} + \arctan\left(\frac{y}{x}\right), \tag{4.8}$$

where y is the position of the slit and x the distance between the slit track and the incoming beam. The slit can be moved by 100 steps of 0.5 mm each. Inserting equation 4.8 in equation 4.7 and solving for λ yields

$$\begin{aligned}\lambda &= d(\sin\vartheta_{out} - \sin\vartheta_{in}) \\ &= d\left(\sin\left(\frac{\pi}{2} + \arctan\left(\frac{y}{x}\right) - \vartheta_{in}\right) - \sin\vartheta_{in}\right) \\ \Leftrightarrow \lambda(y) &= d\left(\cos\left(\arctan\left(\frac{y}{x}\right) - \vartheta_{in}\right) - \sin\vartheta_{in}\right).\end{aligned} \tag{4.9}$$

With $d = 1.667\,\mu\text{m}$, $\vartheta_{in} = (30 \pm 0.5)°$ and $x = (16 \pm 2)$ mm, it is

$$\lambda(y) = 1.667\left[\cos\left(\arctan\left(\frac{y \pm 1\text{ cm}}{16 \pm 2\text{ cm}}\right) - 0.523 \pm 0.009\right) - \sin(0.523 \pm 0.009)\right]\text{nm}. \tag{4.10}$$

Similar to equation 4.4, equation 4.10 can be used to convert the position of the slit into the corresponding wavelength, which is necessary for the first measurements (see section 5). The errors on d, ϑ_{in}, x and y propagate into the error on the wavelength according to

$$\sigma_\lambda^2 = \left(\frac{\lambda}{d}\cdot\sigma_d\right)^2 + d^2\sin^2\left[\arctan\left(\frac{y}{x}\right) - \vartheta_{in}\right]\cdot\left(\frac{xy}{x^2+y^2}\right)^2 \times\left[\left(\frac{\sigma_y}{y}\right)^2 + \left(\frac{\sigma_x}{x}\right)^2\right] + d^2\cos^2\vartheta_{in}\cdot\sigma_{\vartheta_{in}}^2. \tag{4.11}$$

4.3. Complete set-up

Figure 4.7 shows the final set-up, still without the reference light source (compare figure 4.1).

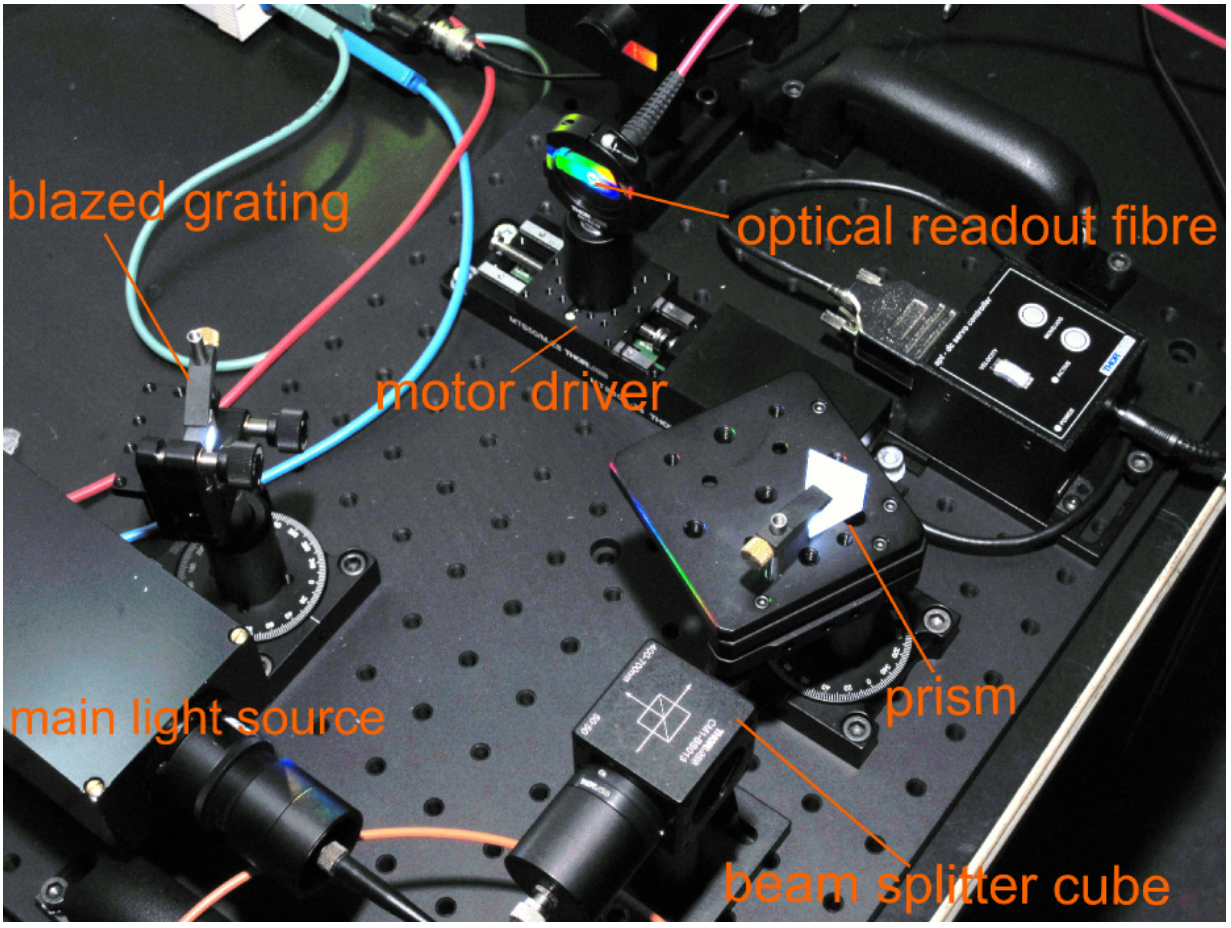

Figure 4.7.: Final set-up (figure taken from [4]).

The main light source box on the left contains the LED and the condenser mounted to it. The light is guided to the beam splitter by an optical fiber, where it is split into two perpendicular beams. A slit mounted on a motorized stage can be moved along the two created spectra, selecting a wavelength. For further information on the practical set-up see [4].

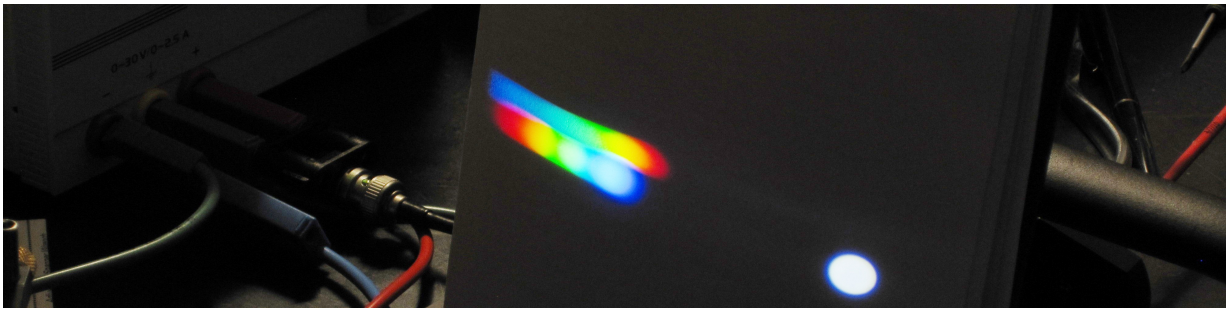

Figure 4.8.: spectra produced by the prism (above) and the grating (below)

The spectra of grating and prism can be regarded one upon the other. By adjusting the height of the slit, the respective spectrum is selected.

5. First results

In order to test a silicon photomultiplier with the test stand, the light has to be pulsed. As the pulsed electronic for the LED is still in development, only the PIN diode is used for the first test. The current in the PIN diode is measured with a picoamperemeter and plotted against the position of the slit, which can be converted into the corresponding wavelength. Figure 5.1(a) (grating) and figure 5.1(b) (prism) show the plots of the first measurements, including noise.

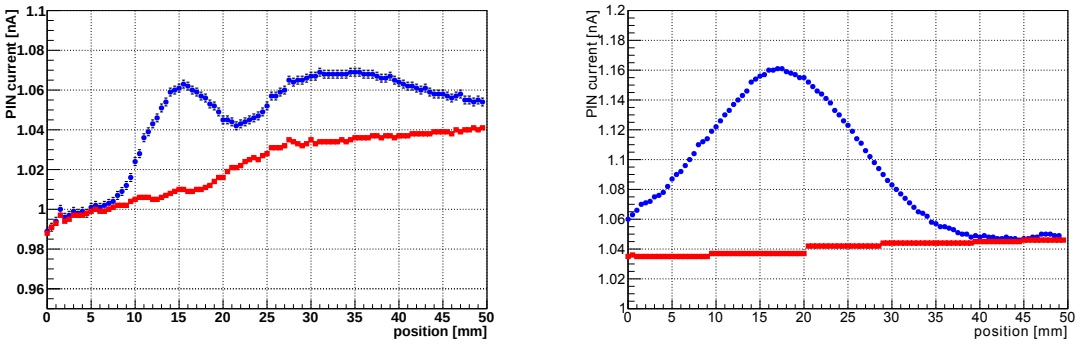

(a) Signal (blue curve) and noise (red curve) for the grating.

(b) Signal (blue curve) and noise (red curve) for the prism.

Figure 5.1.: The first measurements.

Figure 5.2 shows the noise-corrected signals (the difference between signal and noise) for both grating and prism. For both, the PIN current is in the order of magnitude of 100 pA. There is a pronounced structure visible, which means that the light intensity varies across the spectrum. The errors on the PIN current are calculated by error propagation out of the errors on signal and noise, estimating $\sigma_{signal} = 2\,\mathrm{pA}$ and $\sigma_{noise} = 1\,\mathrm{pA}$.
Figure 5.3 shows the same data as figure 5.2, after the conversion from position to wavelength, using equations 4.4 and 4.10 respectively.
The measurements are taken in slightly different wavelength ranges, as the two spectra are not exactly at the same position. The prism does not seem to be optimally adjusted, as half of the spectrum is cut off. The shaded areas in figure 5.3 display the systematic errors on the wavelength caused by the uncertainty of the positions and angles in the set-up (see error calculation in sections 4.1 and 4.2). This systematic is extremely large for the prism, as the deflection angle gets very large for the blue range (see figure 3.4).
In order to minimize the systematic errors, the exactness of these quantities has to be improved by a more precise adjustment. The reference light source will later on facilitate the conversion from slit position to wavelength.
Figure 5.4 shows the photon flux calculated from the PIN current (see [4]). This plot shows, that the test stand is working both for the grating and for the prism. The intensities differ, but are both sufficient for the intended purpose.
Up to 90 photons were detected per 100 ns, which is well inside the dynamical range of silicon photomultipliers currently used. Still, it would be better to pulse the LED, in

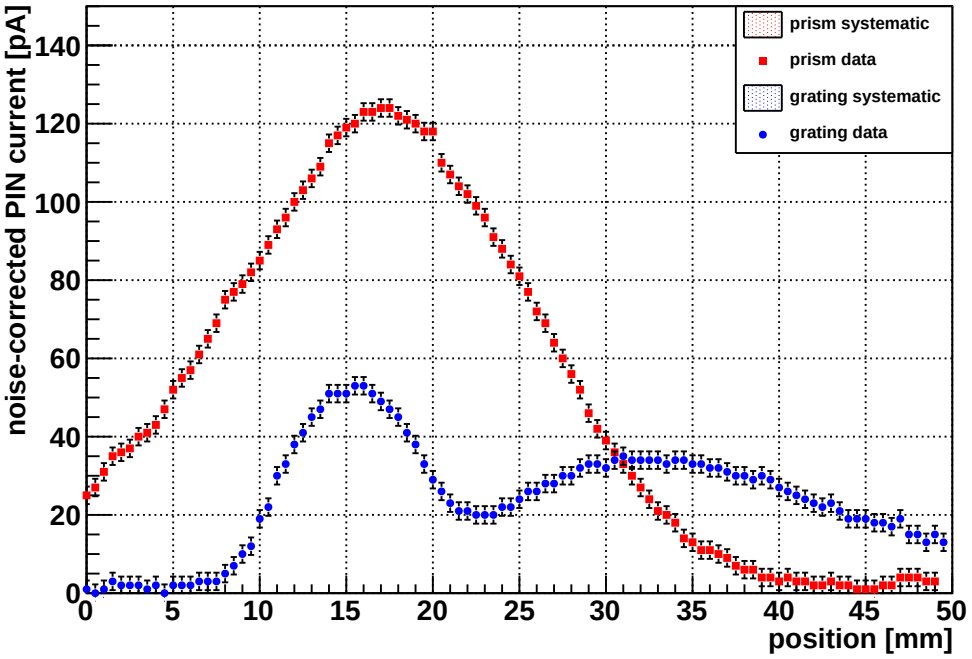

Figure 5.2.: The noise-corrected PIN currents.

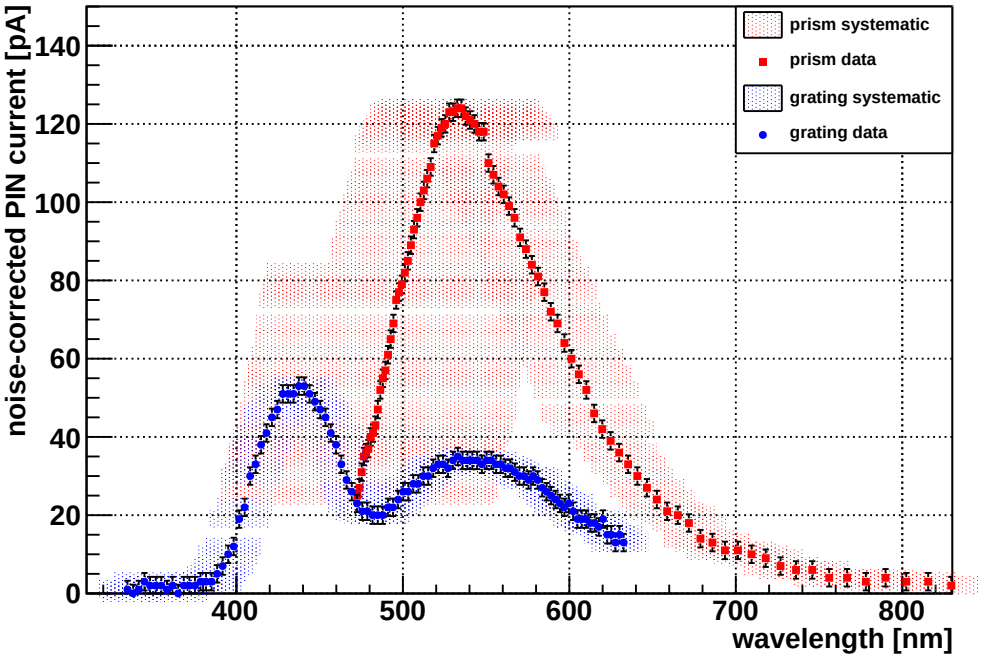

Figure 5.3.: Same data as figure 5.2, after the conversion from position to wavelength.

order to test the immediate response of the silicon photomultiplier to the incoming light. However, the construction of a pulsed light source is not trivial for a current of 700 mA, which is needed for the LED used in this set-up.

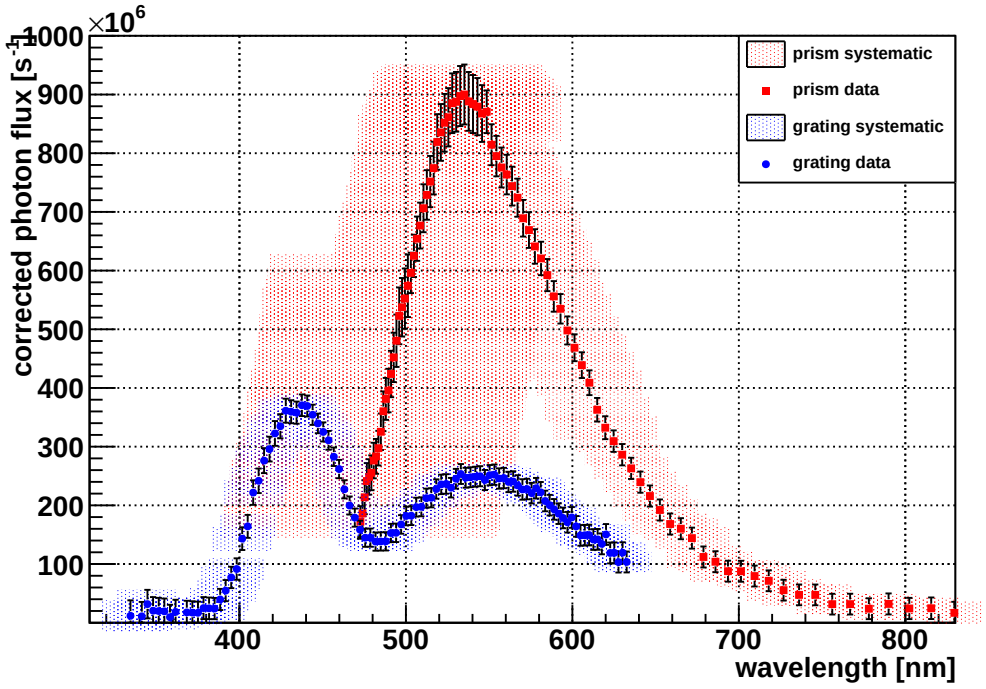

Figure 5.4.: Corrected photon flux. The quantum efficiency of the PIN diode has been applied as a correction factor (see [6]).

6. Conclusion and outlook

We built the test stand as described in [4] according to the concept presented here. While at first we had planned to use two prisms as shown in figure A.1, we later decided to use only one, which is easier to handle than the combination. Both the version with the grating and the version with the prism work and we were already able to take a first measurement with the PIN diode. In both handling and measurement results, the grating seems to be the better solution, although the intensity is higher for the prism.
The calculations in this thesis are the foundation for the test stand. They permit a conversion of the slit position on the motorized stage into the corresponding wavelength.
With the simulation I wrote, the path of light through different combinations of prisms can be calculated and displayed, as can be seen in the plots in section D. It thus serves to illustrate and test possible arrangements of prisms.
The first measurements show that the test stand is working, although the systematic error on the calculated wavelength is still very large. In order to minimize this systematic, the exactness of the measurement of the distances and angles in the set-up has to be increased.
The reference light source is already designed, but still in construction. It is therefore missing in the set-up. Plus, the light of the LED shall be pulsed in order to test a silicon photo multiplier with the constructed test stand. This pulsed electronic is still to be designed.
For a fully-automatic use of the test stand, a control program is needed that allows the control of the motorized stage and the read-out of both the PIN diode and the silicon photomultiplier, as well as the pulsing of the LED and the reference light source.

A. Alternative set-up

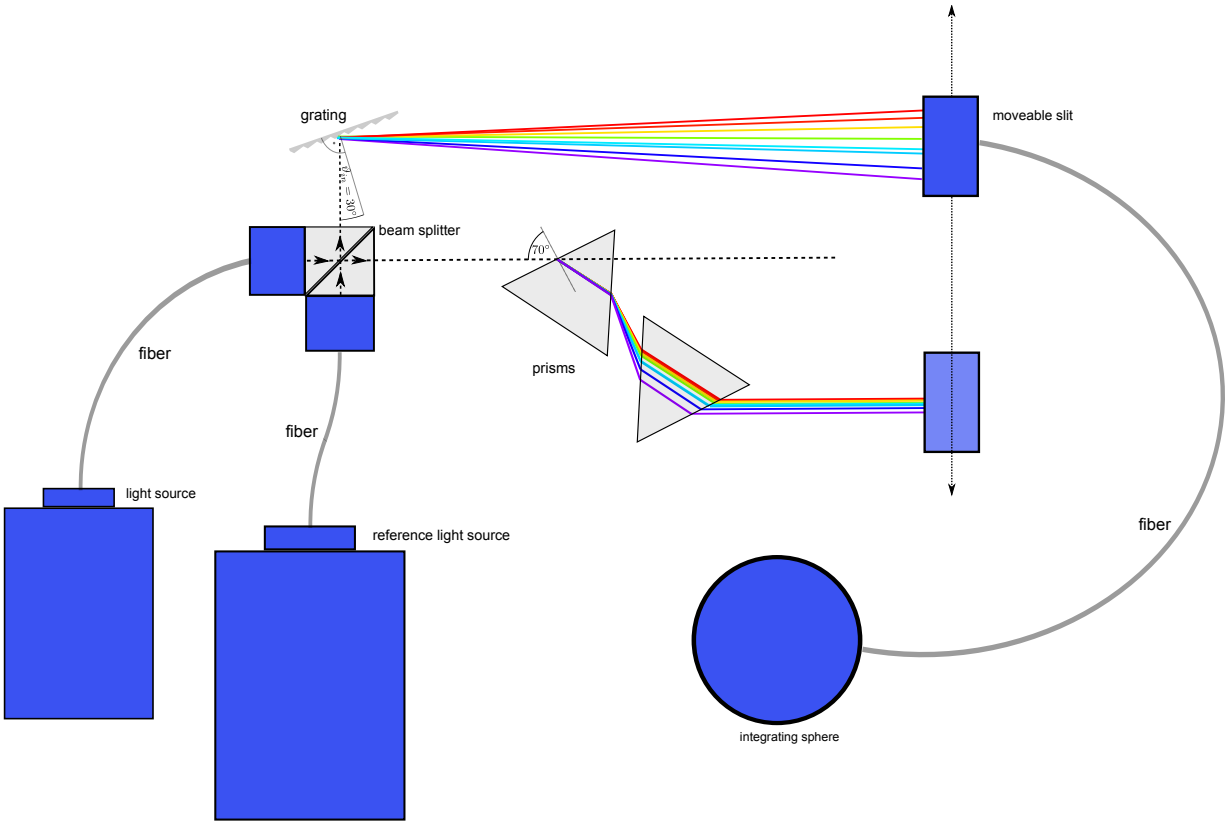

Figure A.1.: Sketch of the set-up with two prisms.

B. Calculations

Replacing α and β in equation 3.22 with their definitions yields

$$1 \cdot \pi = \frac{2\pi d}{\lambda} \cos\left(\frac{\vartheta_{out} + \vartheta_{in}}{2}\right) \sin\left(\frac{\vartheta_{out} - \vartheta_{in}}{2}\right). \tag{B.1}$$

Using

$$\cos(a+b) = \cos a \cdot \cos b - \sin a \cdot \sin b, \tag{B.2}$$

and

$$\sin(a-b) = \sin a \cdot \cos b - \cos a \cdot \sin b, \tag{B.3}$$

this is

$$\begin{aligned}\frac{\lambda}{2d} = &\left[\cos\left(\frac{\vartheta_{out}}{2}\right)\cos\left(\frac{\vartheta_{in}}{2}\right) - \sin\left(\frac{\vartheta_{out}}{2}\right)\sin\left(\frac{\vartheta_{in}}{2}\right)\right] \\ &\cdot \left[\sin\left(\frac{\vartheta_{out}}{2}\right)\cos\left(\frac{\vartheta_{in}}{2}\right) - \cos\left(\frac{\vartheta_{out}}{2}\right)\sin\left(\frac{\vartheta_{in}}{2}\right)\right].\end{aligned} \tag{B.4}$$

Expanding yields

$$\begin{aligned}\frac{\lambda}{2d} = &\left[\cos\left(\frac{\vartheta_{out}}{2}\right)\sin\left(\frac{\vartheta_{out}}{2}\right)\right] \cdot \overbrace{\left[\sin^2\left(\frac{\vartheta_{in}}{2}\right) + cos^2\left(\frac{\vartheta_{in}}{2}\right)\right]}^{=1} \\ &- \left[\cos\left(\frac{\vartheta_{in}}{2}\right)\sin\left(\frac{\vartheta_{in}}{2}\right)\right] \cdot \underbrace{\left[\sin^2\left(\frac{\vartheta_{out}}{2}\right) + cos^2\left(\frac{\vartheta_{out}}{2}\right)\right]}_{=1},\end{aligned} \tag{B.5}$$

which is

$$\frac{\lambda}{2d} = \cos\left(\frac{\vartheta_{out}}{2}\right)\sin\left(\frac{\vartheta_{out}}{2}\right) - \cos\left(\frac{\vartheta_{in}}{2}\right)\sin\left(\frac{\vartheta_{in}}{2}\right). \tag{B.6}$$

Utilizing

$$\sin a \cdot \cos a = \frac{1}{2}\sin(2a), \tag{B.7}$$

yields

$$\frac{\lambda}{2d} = \frac{1}{2}(\sin\vartheta_{out} - \sin\vartheta_{in}). \tag{B.8}$$

This can be resolved, yielding

$$\vartheta_{out} = \arcsin\left(\frac{\lambda}{d} + \sin\vartheta_{in}\right), \tag{B.9}$$

which is

$$\lambda = d(\sin\vartheta_{out} - \sin\vartheta_{in}). \tag{B.10}$$

C. Wavelength dependency of N-SF11 glass

wavelength /nm	refractive index
706.5	1.77119
656.3	1.77596
643.8	1.77732
632.8	1.77860
589.3	1.78446
587.6	1.78472
546.1	1.79192
486.1	1.80651
480.0	1.80841
435.8	1.82533
404.7	1.84235

Table C.1.: The refractive index of N-SF11 glass varies with the wavelength.

D. Prism simulation

Using two parallel prisms, a spectrum of parallel light can be produced in direction of the incoming beam (figure D.1, see also section 3.1.2), which is another possibility for the set-up. Figure A.1 in section A shows the set-up featuring two prisms. The way the prisms are positioned in the simulation, the spectrum would be 3.3 mm wide.

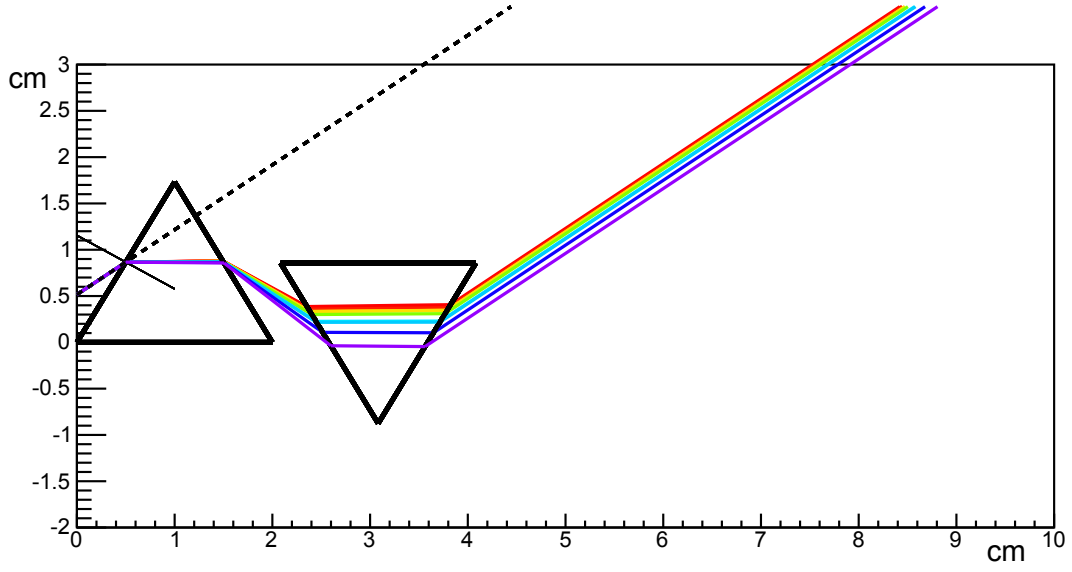

Figure D.1.: A beam of light traversing two prisms.

However, the adjustment of the prisms is problematic. Plus, the produced spectrum is narrow, which reduces the spectral resolution.
A third possibility would be to position a mirror behind one prism, so as to find the spectrum again in direction of the incident beam (figure D.2). For the width of the spectrum, equation 4.1 is valid here, too.
As $\sin\alpha$ in $\sin\alpha = n\sin\beta$ can not be greater than 1, no refraction is possible when β exceeds a critical angle $\beta = \arcsin(\frac{1}{n})$. This called total reflection (see blue and violet ray).

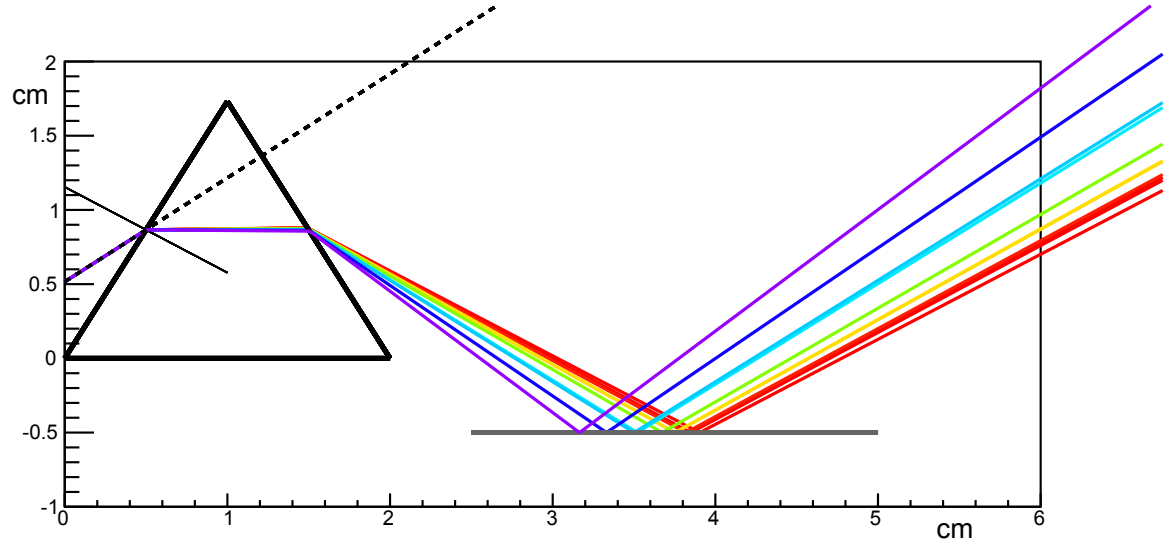

Figure D.2.: A beam of light reflected by a mirror after traversing a single prism.

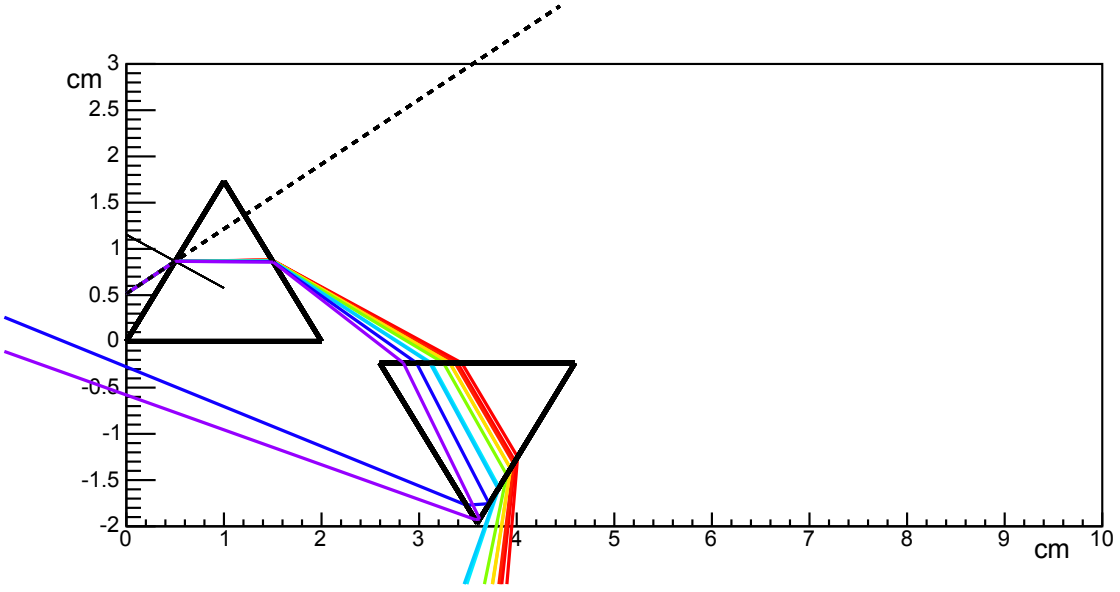

Figure D.3.: total reflection

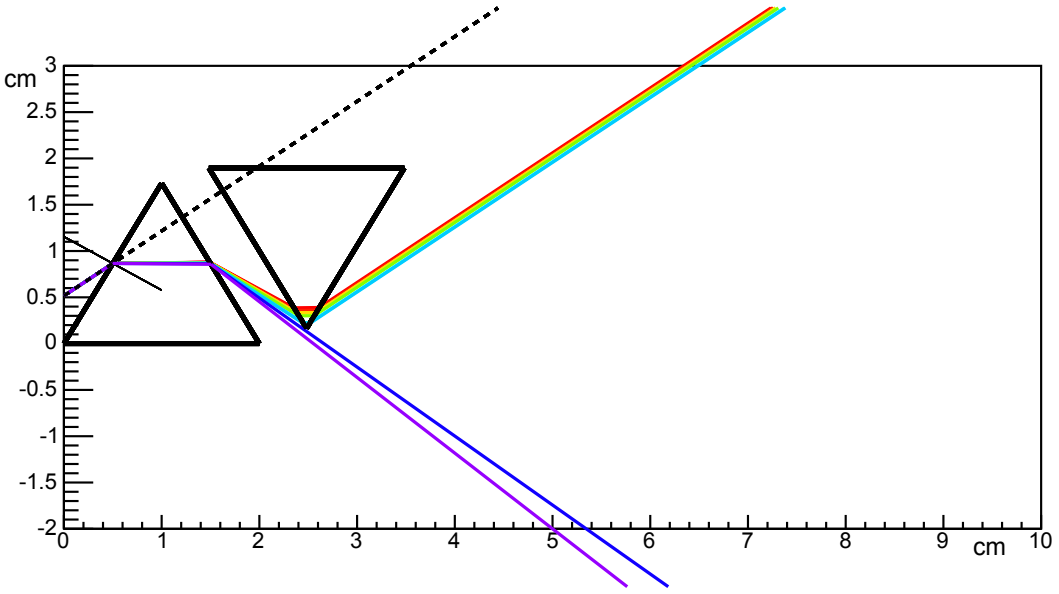

Figure D.4.: The second prism has to be positioned carefully, ensuring that the whole spectrum fits on one side.

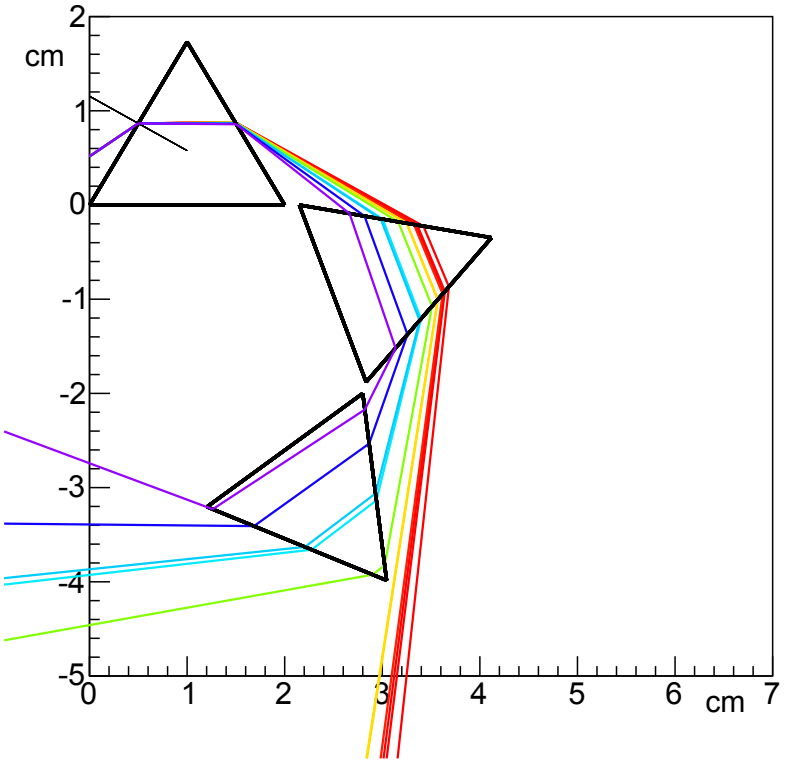

Figure D.5.: With three prisms the spectrum can be turned by 180°. The prisms used in the scope of the thesis, however, disperse too strongly or are too small for the spectrum.

Bibliography

[1] Prof. Dr. Martin Erdmann. *Experimentalphysik III.* lecture notes on experimental physics III, WS2008/09, RWTH Aachen. 2008.

[2] Richardson Gratings. *The physics of diffraction gratings.* `http://gratings.newport.com/library/handbook/chapter2.asp`. 2005.

[3] F. und L. Pedrotti; Werner Bausch; Hartmut Schmidt. *Optik - Eine Einführung.* Prentice Hall, 1996.

[4] Marcia Lins. *Construction and testing of a tunable light source for characterisation of Silicon Photomultipliers.* Bachelor thesis, RWTH Aachen. 2010.

[5] The Center for Occupational Research and Development. *Gratings.* `http://cord.org/cm/leot/course06_mod09/mod06_09.htm`. 1988.

[6] Jan-Frederik Schulte. *Studies of SiPM properties using an integrating sphere.* Bachelor thesis, RWTH Aachen. 2010.

[7] SphereOptics. *Integrating Sphere - Design and Applications.* `http://www.sphereoptics.com/assets/sphere-optic-pdf/sphere-technical-guide.pdf`. 2007.

[8] Julian Stangl. *lecture on Spectroscopy and Structural Analysis - exercise on blazed grid, University of Linz.* `http://www.hlphys.uni-linz.ac.at/hl/lva/vorlesung_spektroskopie_WS200910/ex5_sol5.pdf`. 2009.